American Mineralogist, Volume 105, pages 627–651, 2020

MSA Centennial Symposium

An evolutionary system of mineralogy. Part I: Stellar mineralogy (>13 to 4.6 Ga)

Robert M. Hazen[1,*] and Shaunna M. Morrison[1]

[1]Earth and Planets Laboratory, Carnegie Institution for Science, 5251 Broad Branch Road NW, Washington, DC 20015, U.S.A.

Abstract

Minerals preserve records of the physical, chemical, and biological histories of their origins and subsequent alteration, and thus provide a vivid narrative of the evolution of Earth and other worlds through billions of years of cosmic history. Mineral properties, including trace and minor elements, ratios of isotopes, solid and fluid inclusions, external morphologies, and other idiosyncratic attributes, represent information that points to specific modes of formation and subsequent environmental histories—information essential to understanding the co-evolving geosphere and biosphere. This perspective suggests an opportunity to amplify the existing system of mineral classification, by which minerals are defined solely on idealized end-member chemical compositions and crystal structures. Here we present the first in a series of contributions to explore a complementary evolutionary system of mineralogy—a classification scheme that links mineral species to their paragenetic modes.

The earliest stage of mineral evolution commenced with the appearance of the first crystals in the universe at >13 Ga and continues today in the expanding, cooling atmospheres of countless evolved stars, which host the high-temperature (T > 1000 K), low-pressure ($P < 10^{-2}$ atm) condensation of refractory minerals and amorphous phases. Most stardust is thought to originate in three distinct processes in carbon- and/or oxygen-rich mineral-forming stars: (1) condensation in the cooling, expanding atmospheres of asymptotic giant branch stars; (2) during the catastrophic explosions of supernovae, most commonly core collapse (Type II) supernovae; and (3) classical novae explosions, the consequence of runaway fusion reactions at the surface of a binary white dwarf star. Each stellar environment imparts distinctive isotopic and trace element signatures to the micro- and nanoscale stardust grains that are recovered from meteorites and micrometeorites collected on Earth's surface, by atmospheric sampling, and from asteroids and comets. Although our understanding of the diverse mineral-forming environments of stars is as yet incomplete, we present a preliminary catalog of 41 distinct natural kinds of stellar minerals, representing 22 official International Mineralogical Association (IMA) mineral species, as well as 2 as yet unapproved crystalline phases and 3 kinds of non-crystalline condensed phases not codified by the IMA.

Keywords: Classification, mineral evolution, mineral ecology, natural kinds, vapor deposition, condensation, astromineralogy, stardust, diamond, graphite, corundum, moissanite, hibonite, amorphous phases

"*The science of Mineralogy has made rapid progress in the past six years; chemistry has opened to us a better knowledge of the nature and relations of compounds; and philosophy has thrown new light on the principles of classification. To change is always seeming fickleness. But not to change with the advance of science, is worse; it is persistence in error.*"

James Dwight Dana, *System of Mineralogy*, Third Edition, 1850, p. 5

Introduction

Mineral diversity and distribution have evolved through almost 14 billion years of cosmic history, as a succession of physical, chemical, and ultimately biological processes led to the selection and concentration of mineral-forming elements in varied pressure-temperature-composition environments. As such, minerals and other condensed phases bear vivid testimony to the ancient origins and storied evolution of diverse worlds, both in our solar system and in star systems far beyond. A central objective of Earth and planetary sciences is to tease out those histories from the rich, revealing mineralogical evidence left behind.

The present system of mineral classification of the International Mineralogical Association's Commission on New Minerals, Nomenclature and Classification (IMA, CNMNC; e.g., Burke 2006; Mills et al. 2009; Schertl et al. 2018) is based on pure end-member chemical compositions and idealized crystal structures—the minimum information necessary to distinguish between any two species. Such a coherent and reproducible framework is essential for the field of mineralogy, and it will remain the foundation for mineral nomenclature and classification for decades to come. However, by design the IMA classification system does not incorporate the idiosyncratic compositional variations, distinctive physical properties, and diverse morphological characteristics of minerals

* E-mail: rhazen@ciw.edu; Orcid 0000-0003-4163-8644.

0003-004X/20/0005–627$05.00/DOI: https://doi.org/10.2138/am-2020-7173

and other condensed phases formed under varying environmental conditions at different historical stages of the cosmos (e.g., Santana 2019). Therefore, we have the opportunity to build on the present system of mineralogy, to capture more fully the evolving mineralogical diversity of Earth and other worlds through deep time.

We propose a complementary "evolutionary classification system" of minerals, which catalogs minerals by coupling species with their paragenetic modes. Accordingly, we adopt a binomial nomenclature, with a mineral name preceded by a descriptor of the paragenetic mode, such as "*impact stishovite*," "*pegmatitic hydroxylapatite*," or "*biogenic pyrite*." The system is divided into chronological parts, each representing a different stage of mineral evolution (Hazen et al. 2008; Hazen and Ferry 2010). In Part I, we consider stellar mineralogy and the earliest condensed phases in the cosmos, to be followed by interstellar and nebular mineralogy (Parts II and III), planetesimal mineralogy (Parts IV and V), and a series of subsequent contributions focused on planetary processes. Within each part, minerals are arranged according to the Dana System: Native Elements, followed by Sulfides, Oxides, and Hydroxides, etc. (J.D. Dana et al. 1973; Gaines et al. 1997; see http://www.webmineral.com, accessed 28 September 2019).

We employ IMA-approved mineral names for the great majority of species. However, the evolutionary system of mineralogy deviates from IMA nomenclature in three significant ways (Hazen 2019). First, by employing a binomial nomenclature, we split many common minerals into multiple kinds based on their distinctive paragenetic modes. Thus, in our system diamond formed by low-pressure condensation in a stellar atmosphere (e.g., *AGB diamond*; see below) differs from diamond formed by shock alteration of carbon-rich material (*impact diamond*), or crystallized at high pressure and temperature in Earth's mantle (e.g., *Type 1 diamond*).

On the other hand, in some instances, two or more IMA species would be lumped because they form by a single process in a continuous phase space. The occurrence of zoned minerals within complex compositional space, for example, in the pyroxene, amphibole, mica, and tourmaline groups, often results in multiple IMA species being present in a single mineral grain (e.g., dravite-schorl in zoned tourmaline crystals; Grew et al. 2015). In these instances, we lump two or more compositional end-member mineral species into a single natural kind. We also catalog various non-crystalline condensed phases as natural kinds—materials important in planetary evolution, even though they are not typically assigned official mineral names by the present IMA procedures.

This contribution is the first in a planned series of publications on an evolutionary system of mineralogy that will examine chronologically the emerging diversity and distribution of condensed phases found on Earth, as well as on other planets, moons, and nebular environments. Here we explore stardust—remnants from the earliest episodes of mineral evolution. Stellar mineralogy, or "astromineralogy" (e.g., DePew et al. 2006; A.P. Jones 2007), encompasses all solid phases that form in the atmospheres of stars—mineralization that commenced more than 13 billion years ago, long before the formation of our solar nebula. At least 41 different natural kinds of stellar minerals, representing 22 IMA-approved mineral species, two crystalline phases not yet approved by the IMA, and three non-crystalline phases (Table 1), formed primarily from 11 relatively abundant chemical elements that emerged from stellar nucleosynthesis—C, N, O, Mg, Al, Si, S, Ca, Ti, Cr, and Fe (e.g., Clayton 1983; Rolfs and Rodney 2005; Schatz 2010; Fig. 1a). The expanding, cooling gaseous envelopes of aged stars, characterized by high-temperature (>1000 K) and low-pressure ($<10^{-2}$ atm) condensation of a few refractory phases (Fig. 1b), represent the most ancient mineral-forming environments in the cosmos.

On the nature of stardust

Stellar minerals must have first formed within a few hundred million years of the Big Bang, as temperatures in the expanding gaseous envelopes of supernovae and early generations of other highly evolved stars (Abel et al. 2002; Robertson et al. 2015; Bowman et al. 2018) fell significantly below the maximum ~1700 K condensation temperature of diamond in a carbon-rich gas at ~10^{-4} atm (Lodders and Amari 2005). Varied nano- and microcrystalline phases, collectively called the "ur-minerals" (Hazen et al. 2008), represent the earliest condensed matter in the history of the universe—the true beginnings of cosmic mineralogy.

The first evidence for mineral formation around stars came from observations of distinctive infrared absorption features from the dust-rich expanding envelopes of planetary nebulas and supernovae (Gillett et al. 1968; Woolf and Ney 1969; Treffers and Cohen 1974; see Boulanger et al. 2009 and references therein). Donald Clayton subsequently suggested that presolar stellar condensates may be preserved in meteorites and should have significant isotopic anomalies compared to solar abundances (Clayton 1975, 1978; Clayton and Ward 1978)—speculations confirmed by laboratory discoveries in the late 1980s (Lewis et al. 1987; Bernatowicz et al. 1987; Zinner et al. 1987; Amari et al. 1990). These ancient specks of stardust have become the focus of increasingly intense study by both mineralogists and astrophysicists (e.g., Clayton and Nittler 2004; Lodders and Amari 2005; Lugaro 2005; Davis 2011, 2014; Zinner 2014; Nittler and Ciesla 2016; and references therein).

Presolar grains are present in the least processed extraterrestrial materials, including meteorites and micrometeorites collected on Earth's surface (e.g., Yada et al. 2008), interplanetary dust particles collected from Earth's upper atmosphere by high-altitude aircraft (Hodge 1961; Dermott and Liou 1994; Messenger 2002), and samples of comet Wild-2 returned by NASA's *Stardust* mission (e.g., McKeegan et al. 2006; Stadermann et al. 2008). They are identified by their highly anomalous isotopic compositions, compared to materials that formed in the solar system, which point to an origin in the turbulent winds and/or explosions of previous generations of evolved stars. A significant suite of micro- and nanophases are now recognized by their distinctive chemistries, isotopic compositions, and morphologies—features that point to origins in various carbon- and/or oxygen-rich stellar environments (Table 1). Each individual presolar grain formed during a given time interval in a given evolved star and thus preserves a fossil memory of the physical and chemical conditions of its formation environment (Bernatowicz et al. 2003; Zinner 2014; Takigawa et al. 2018).

Studying stellar minerals is challenging on several fronts as a consequence of their diminutive scale. All stellar mineral grains are small, ranging from multi-micrometer-scale grains of graphite and moissanite (SiC) with many trillion atoms to nano-diamonds with fewer than 1000 atoms per particle (e.g., Lugaro 2005; Davis 2011). The first identified and best-studied presolar phases (SiC

TABLE 1. Diagnostic properties of stardust minerals and other condensed phases

Species (Formula)	Natural kind	Characteristics	References
		Native Elements	
Diamond (C)	AGB diamond	high $^{12}C/^{13}C$; low $^{14}N/^{15}N$; possibly high ^{22}Ne	1,2
	SN-II diamond	low $^{12}C/^{13}C$; possibly high Xe	2,3
Graphite (C)	AGB graphite	high $^{12}C/^{13}C$; high Zr, Mo, Ti	4–8
	SN-II graphite	low $^{14}N/^{15}N$; high $^{18}O/^{16}O$; ^{26}Mg, ^{44}Ca, and ^{49}Ti	7,9,10
	CNova graphite	very low $^{12}C/^{13}C$; high $^{30}Si/^{28}Si$; high ^{22}Ne	8,11,12
Amorphous Carbon (C)	Stellar amorphous C	amorphous to electron diffraction; anomalous $^{12}C/^{13}C$	13,14
Iron (Fe)	SN-II iron	nano-scale inclusions in SN-II graphite	4,5,10,15–17
Taenite (Fe,Ni)	SN-II taenite	nano-scale inclusions in SN-II graphite	4,5,10,15–17
Ruthenium (Ru)	SN-II ruthenium	nano-scale inclusion in SN-II graphite	5,15
Osmium (Os)	SN-II osmium	nano-scale inclusion in SN-II graphite	5,15
Other Native Elements (?)	[Nickel, Ni]	nano-scale inclusion in graphite, alloyed with Fe	18,19
		Carbides	
Moissanite (SiC)	AGB moissanite	typically low $^{12}C/^{13}C$; often with elevated Zr, Mo, Ti	19–29
	SN-II moissanite	low $^{14}N/^{15}N$; high $^{29}Si/^{28}Si$ & $^{30}Si/^{28}Si$; elevated ^{26}Mg; ^{44}Ca	30–33
	CNova moissanite	low $^{12}C/^{13}C$; high $^{30}Si/^{28}Si$; high ^{22}Ne	11,31,34
Khamrabaevite (TiC)	AGB khamrabaevite	enriched in *s*-process elements V, Zr, Mo, and Ru	4,6,35
	SN-II khamrabaevite	grains embedded in graphite; enriched in V, but not Zr, Mo, Ru	17,36,37
Mo-Zr carbide [(Mo,Zr)C]	AGB Mo-Zr carbide	nano-inclusions in AGB graphite; usually with Ti	4,37
Cohenite (Fe_3C)	SN-II cohenite	nano-inclusions in SN-II graphite	38
Iron Carbide [$(Fe,Cr)_7C_3$]	SN-II iron carbide	nano-inclusions in SN-II graphite	5
Other Carbides (?)	[Ti-Al carbide]	subgrains in SN-II graphite	37
		Silicides	
$(Fe,Ni)_2Si$	~[$(Fe,Ni)_2Si$]	nano-inclusions in SiC; unknown structure and composition	19
$(Fe,Ni)_3Si$	~[$(Fe,Ni)_3Si$]	nano-inclusions in SiC; unknown structure and composition	19
		Phosphides	
Schreibersite (Fe_3P)	[schreibersite]	Unconfirmed, but predicted to be a stellar condensate	39
		Nitrides	
Nierite (Si_3N_4)	SN-II nierite	low $^{14}N/^{15}N$; and low $^{30}Si/^{28}Si$	33,40,41
Other Nitrides (?)	[Ti(N,C)]	local concentrations in SiC	16,42
	[(Mg,Al)N]	local concentrations in SiC	16,42
	[Al nitride]	local concentrations in SiC	19,43
		Sulfides	
Oldhamite (CaS)	AGB oldhamite	nano-scale inclusions in moissanite	39,44
Troilite (FeS)	SN-II (?) troilite	nano-scale inclusions in graphite, negative $\delta^{33}S$ and ^{34}S	12
Other Sulfides (?)	[Niningerite, MgS]	Unconfirmed, but predicted to be a stellar condensate	39
		Oxides	
Corundum (Al_2O_3)	AGB corundum	typically with high $^{17}O/^{16}O$; low $^{18}O/^{16}O$	45–50
	SN-II corundum	low $^{17}O/^{16}O$; high $^{18}O/^{16}O$; ^{26}Mg,^{44}Ca	47,50
	CNova corundum	very high $^{17}O/^{16}O$, low $^{18}O/^{16}O$	50
Amorphous Al_2O_3	AGB amorphous Al_2O_3	amorphous in TEM; high $^{17}O/^{16}O$; low $^{18}O/^{16}O$; ^{26}Mg	49,51
Eskolaite (Cr_2O_3)	SN-II eskolaite	occurs as subgrains in SN-II graphite	18
Rutile (TiO_2)	AGB TiO_2	high $^{17}O/^{16}O$ [structure not yet confirmed]	50,53
	SN-II rutile	high $^{18}O/^{16}O$; occurs as subgrains in SN-II graphite	37,42
Magnetite (Fe_3O_4)	AGB magnetite	elevated $^{17}O/^{16}O$; occurs as subgrains in graphite	18,54
Spinel ($MgAl_2O_4$)	AGB spinel	high $^{17}O/^{16}O$; low $^{18}O/^{16}O$	47,55,56
	SN-II spinel	high $^{18}O/^{16}O$, low ^{25}Mg, and high ^{26}Mg	50,56
	CNova spinel	extreme enrichments in ^{17}O, ^{25}Mg, and ^{26}Mg	56
Chromite ($Fe^{2+}Cr_2O_4$)	AGB chromite	high $^{17}O/^{16}O$; low $^{18}O/^{16}O$	55,57
Hibonite [$(Ca,Ce)(Al,Ti,Mg)_{12}O_{19}$]			
	AGB hibonite	high $^{17}O/^{16}O$; high ^{26}Mg	50,52,58,59
	SN-II hibonite	high $^{18}O/^{16}O$; low ^{25}Mg; high ^{26}Mg	50,52
Other oxides (?)	[Fe oxide]	unknown structure/composition;	60,61
	[Cr oxide]	cubic structure, unknown composition	18
	[Ca-Al oxide]	unknown structure/composition	50
	[Mg chromate]	unknown structure/composition	50
	["hexagonal Al_2O_3."]	unknown structure	51
		Silicates	
Forsterite [$(Mg,Fe)_2SiO_4$]	AGB forsterite	high $^{17}O/^{16}O$	62–67
	SN-II forsterite	low $^{17}O/^{16}O$; high $^{18}O/^{16}O$	68
Enstatite [$(Mg,Fe)SiO_3$]	AGB enstatite	high $^{17}O/^{16}O$	62,69
	SN-II enstatite	normal $^{17}O/^{16}O$; very high $^{18}O/^{16}O$	53,62,69–72
Bridgmanite ($MgSiO_3$)	AGB bridgmanite	high $^{17}O/^{16}O$; probably a post-stellar shocked enstatite grain	73
Amorphous silicate	AGB amorphous Mg-Fe silicate	high $^{17}O/^{16}O$	74–76

Note: In the second column for natural kinds, unconfirmed phases appear in [brackets].

References: 1. Verchovsky et al. 2006; 2. Lewis et al. 2018; 3. Lewis et al. 1987; 4. Bernatowicz et al. 1996; 5. Croat et al. 2005; 6. Bernatowicz et al. 2006; 7. Jadhav et al. 2013; 8. Jadhav et al. 2008; 9. Nittler et al. 1996; 10. Stadermann et al. 2005; 11. Amari et al. 2001c; 12. Haenecour et al. 2016; 13. Stroud et al. 2011; 14. Wopenka et al. 2011b; 15. Croat et al. 2013; 16. Gyngard et al. 2018; 17. Croat et al. 2003; 18. Croat et al. 2008; 19. Hynes et al. 2010; 20. Davis 2011; 21. Stroud et al. 2004a; 22. Hoppe et al. 1995; 23. Amari et al. 2001b; 24. Fujiya et al. 2013; 25. Liu et al. 2017c; 26. Nguyen et al. 2018; 27. Hoppe et al. 1994; 28. Amari et al. 2001a; 29. Hoppe et al. 1997; 30. Croat et al. 2010; 31. Liu et al. 2016; 32. Liu et al. 2018; 33. Lin et al. 2010; 34. José and Hernandez 2007; 35. Bernatowicz et al. 1992; 36. Groopman et al. 2012; 37. Croat et al. 2011; 38. Bernatowicz et al. 1999; 39. Lodders and Amari 2005; 40. Nittler et al. 1995; 41. Hoppe et al. 1996; 42. Groopman and Nittler 2018; 43. Stroud and Bernatowicz 2005; 44. Hynes et al. 2011; 45. Hutcheon et al. 1994; 46. Nittler et al. 1997; 47. Choi et al. 1998; 48. Takigawa et al. 2014; 49. Takigawa et al. 2018; 50. Nittler et al. 2008; 51. Stroud et al. 2004b; 52. Zega et al. 2011; 53. Bose et al. 2010a; 54. Zega et al. 2015; 55. Zega et al. 2014a; 56. Gyngard et al. 2010a; 57. Nittler et al. 2005; 58. Choi et al. 1999; 59. Nittler et al. 2011; 60. Floss et al. 2008; 61. Bose et al. 2010b; 62. Mostefouai and Hoppe 2004; 63. Busemann et al. 2009; 64. Vollmer et al. 2009; 65. Zega et al. 2014b; 66. Nguyen and Messenger 2014; 67. Nittler et al. 2018b; 68. Messenger et al. 2005; 69. Floss and Stadermann 2009; 70. Floss and Stadermann 2012; 71. Vollmer et al. 2013; 72. Nguyen et al. 2016; 73. Vollmer et al. 2007; 74. Kemper et al. 2004; 75. Messenger et al. 2003; 76. Zinner 2014.

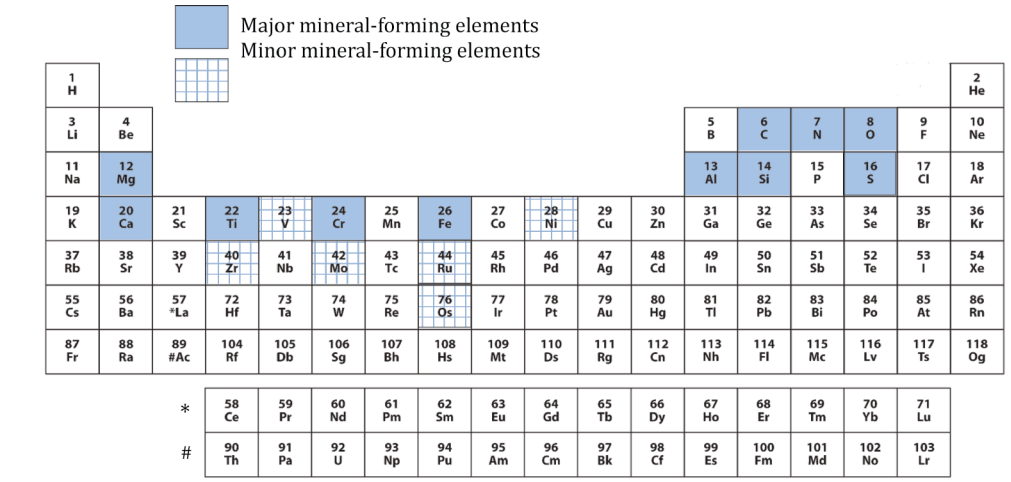

A.

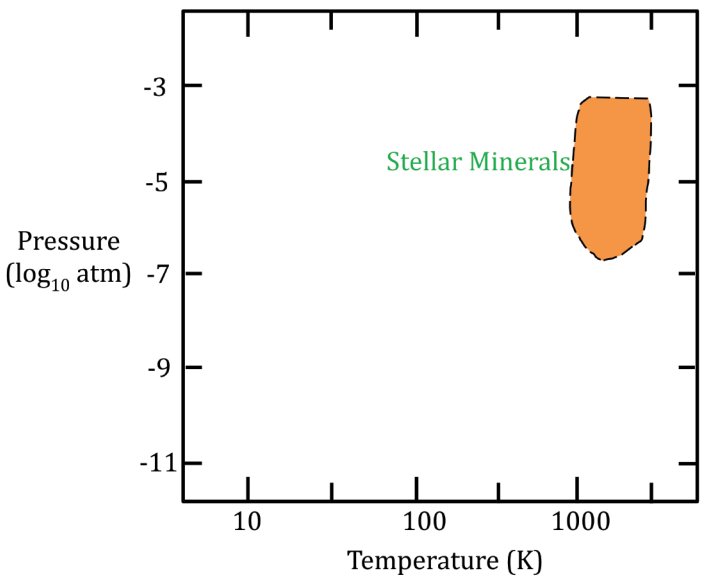

B.

FIGURE 1. Characteristic pressure-temperature-composition regimes of stellar minerals. (**a**) Eleven major mineral-forming elements and six select minor elements commonly found in stardust. (**b**) Estimated pressure-temperature formation ranges of most stellar primary condensate minerals, which formed via relatively low-pressure, high-temperature condensation in the turbulent atmospheres of highly evolved stars. (Color online.)

and C allotropes; Lewis et al. 1987; Bernatowicz et al. 1987; Zinner et al. 1987) are highly refractory and acid-resistant, so they can be isolated from meteorites via acid dissolution of the dominant silicate, metal, and sulfide phases ("burning down a haystack to find a needle"). The development of nanoscale secondary ion mass spectrometry (NanoSIMS) technology later enabled high-resolution (<0.1 μm) isotopic mapping of interplanetary dust and meteorites to identify presolar grains in situ, especially presolar silicates, as these grains are destroyed by the acid dissolution methods (Messenger et al. 2003; Mostefouai and Hoppe 2004; Nagashima et al. 2004; Nguyen and Zinner 2004). Once identified by their anomalous isotopic compositions, presolar grains can be prepared by focused ion beam (FIB) methods and analyzed by transmission electron microscopy (TEM). Such investigations of individual grains are now providing remarkable insights regarding the ancient origins and evolution of stardust (Amari 2014; Zinner 2014; Nittler and Ciesla 2016).

At least 22 different IMA-approved mineral species and five other phases have been confirmed as stellar minerals (Table 1). However, the varied grains in stardust, including several amorphous or glassy phases, display a wide diversity of observed attributes, including distinctive elemental and isotopic compositions, external morphologies, and microstructures that point to at least three major paragenetic modes, resulting in a list of natural kinds of condensed stellar phases significantly greater than the modest list of official mineral species. In this context, grains with similar isotopic and structural attributes are assumed to have had similar histories, arising in some cases from the same parent stellar environment. An important and as yet poorly constrained aspect of stellar mineralogy is that the temperature-pressure-composition regimes of dust-producing stars differ widely, both from star to star and spatially and temporally within the evolving dynamic atmospheres of any given star. Consequently, suites of these grains will vary significantly, depending on their specific peripatetic stellar histories. In some instances, presolar mineral grains (especially suites of refractory inclusions) appear to represent relatively pristine primary condensates—in essence pure fragments of a specific star. However, other grains

may have experienced subsequent reworking that significantly altered the mineral's elemental and isotopic compositions and/or structural state, both within a dynamic stellar environment and through subsequent nebular processing. As a result, stellar mineralogy, though limited to the most refractory high-temperature phases of cosmically abundant elements, is richly varied in ways that are only gradually coming to light.

On the paragenesis of stellar minerals

Long before the emergence of our solar system and its intriguing diversity of mineral-rich worlds, condensed crystalline and amorphous phases formed abundantly in the ejecta of supernovae and classical novae, as well as in the expanding, cooling gaseous envelopes of highly evolved stars (Mostefouai and Hoppe 2004; Lodders and Amari 2005; Hynes et al. 2010; Davis 2011; Nittler and Ciesla 2016; Nittler et al. 2018a). Here we review stellar environments in which isotopes are synthesized and astrominerals emerge. In the following two sections, we briefly summarize two key aspects of stardust: (1) the nucleosynthetic origins of mineral-forming elements, and (2) the three types of high-temperature stellar environments in which minerals most frequently condense. For detailed discussions of the stellar origins of astrominerals see reviews by Lodders and Amari (2005), Nittler and Dauphas (2006), Davis (2011), Zinner (2014), and Nittler and Ciesla (2016).

Stellar nucleosynthesis and the origins of mineral-forming elements

Minerals on Earth are known to incorporate almost 300 stable or long-lived isotopes of at least 72 chemical elements. Big-Bang Nucleosynthesis (BBN), by contrast, can account for significant quantities of only hydrogen, helium, and lithium (Bertulani 2013, and references therein), though trivial quantities of heavier elements, including carbon, nitrogen, and oxygen, also emerged from BBN (Iocco et al. 2008). Consequently, almost all mineral-forming elements other than hydrogen arose through processes of stellar nucleosynthesis (Burbidge et al. 1957; Cameron 1957; Schatz 2010; Bertulani 2013), which began ~100 Ma after the Big Bang with the first generation of massive stars (Abel et al. 2002; Robertson et al. 2015; Bowman et al. 2018). A variety of nucleosynthetic mechanisms, each of which produces a distinctive pattern of elements and isotopes, contribute significantly to suites of mineral-forming elements and their isotopes in stars (e.g., Truran and Heger 2003; Zinner 2014; Nittler and Ciesla 2016).

Nucleosynthesis in stars is inextricably linked to stellar evolution, which can be characterized as a competition between the inward force of gravitational contraction and the outward force of nuclear fusion reactions. Gravitational compression within stars heats matter to the point where exothermic nuclear fusion reactions occur, providing energy to counteract collapse. When one nuclear fuel source is exhausted, depending on the mass and composition of the stellar core, gravity can cause core contraction until a new stage of fusion reactions commences. The formation of mineral-forming elements and isotopes is summarized below.

• *Hydrogen burning.* Most stellar nucleosynthesis, most of the time, involves "hydrogen burning"—the three-step fusion mechanism that transforms four protons into a ^{4}He nucleus (an α particle), with two protons and two neutrons. All stars spend most of their lives powered by hydrogen burning in their cores—the process that dominates stars on the main sequence of the Hertzsprung-Russell diagram (e.g., L.V. Jones 2009).

• *Helium burning and carbon nucleosynthesis*. As the α particle concentration increases in a star's core, "helium burning" commences, producing ^{12}C through the triple-α process (e.g., Carroll and Ostlie 2017)—a process characteristic of "red giant branch" (RGB) stars. In stars more massive than the Sun, ^{12}C catalyzes additional helium production from protons through the "CNO cycle" (e.g., Limongi and Chieffi 2012; Carroll and Ostlie 2017), while increasing the concentrations of ^{13}C and ^{15}N relative to ^{12}C and ^{14}N. However, these fusion reactions do not generate a significant suite of mineral-forming elements other than carbon.

• *Late-stage fusion processes—most elements to Fe.* Most elements to Fe. Most synthesis of essential elements in stellar minerals occurs during late-stage fusion processes in stars that have left the main sequence. The details of what occurs after core He burning depend critically on the initial mass of the star. For stars less massive than about 8 times that of the Sun, the C-O core remains stable against gravity due to quantum mechanical "electron degeneracy" pressure, but H and He burning continue to produce energy in narrow shells outside the core. A star in this post-RGB stage is referred to as an "asymptotic giant branch" or AGB star, which produces copious amounts of dust that drives strong winds. An AGB star expels much of its dust-rich envelope into interstellar space, temporarily appearing as a spectacular "planetary nebula" before leaving behind its cooling core as a white dwarf star (Fig. 2a). (Note that the misleadingly named "planetary" nebula is not related to planet formation, which occurs in a "solar nebula.")

The nuclear histories and fates of stars greater than ~8 solar masses are even more dramatic. Following He burning, massive stars continue the sequence of burning increasingly heavier fuels in their cores through the "α process" or "α ladder," by which α particles fuse initially with ^{12}C in a stepwise sequence: $^{12}\text{C} \rightarrow {}^{16}\text{O} \rightarrow {}^{20}\text{Ne} \rightarrow {}^{24}\text{Mg} \rightarrow {}^{28}\text{Si}$, etc., to ^{56}Fe, thus producing several of the most abundant mineral-forming isotopes (e.g., L.V. Jones 2009). These and other fusion reactions, including myriad steps during carbon burning, neon burning, oxygen burning, and silicon burning, occur near the end of the lives of AGB stars significantly more massive than the Sun. This increasingly rapid sequence of fusion reactions is responsible for much of the production of isotopes up to ^{60}Zn (e.g., Truran and Heger 2003; Carroll and Ostlie 2017).

• *Core collapse in Type II supernovae.* ^{56}Fe has the highest binding energy of any common nucleus; therefore, it cannot produce energy through fusion reactions and eventually the battle against gravity is lost. Consequently, when the core of a large star becomes enriched in ^{56}Fe, nuclear fusion reactions no longer exert an outward pressure and gravity takes over. The iron core collapses to form either a neutron star or a black hole and the outer layers are ejected in a spectacular Type II supernova explosion (Fig. 2b). The extreme temperatures and pressures of gravitationally induced core collapse result in a cascade of nuclear reactions, producing short-lived isotopes such as ^{26}Al, ^{44}Ti, and ^{49}V, which decay rapidly to stable ^{26}Mg, ^{44}Ca, and ^{49}Ti—diagnostic isotopes preserved in stellar minerals (Clayton 1975; Nittler et al. 1996; Timmes et al. 1996).

• *Slow neutron capture (s-process).* In spite of their importance in producing the major elements of stellar minerals, the fusion processes outlined above generate only about a third of Earth's mineral-forming chemical elements (Johnson 2019). Elements

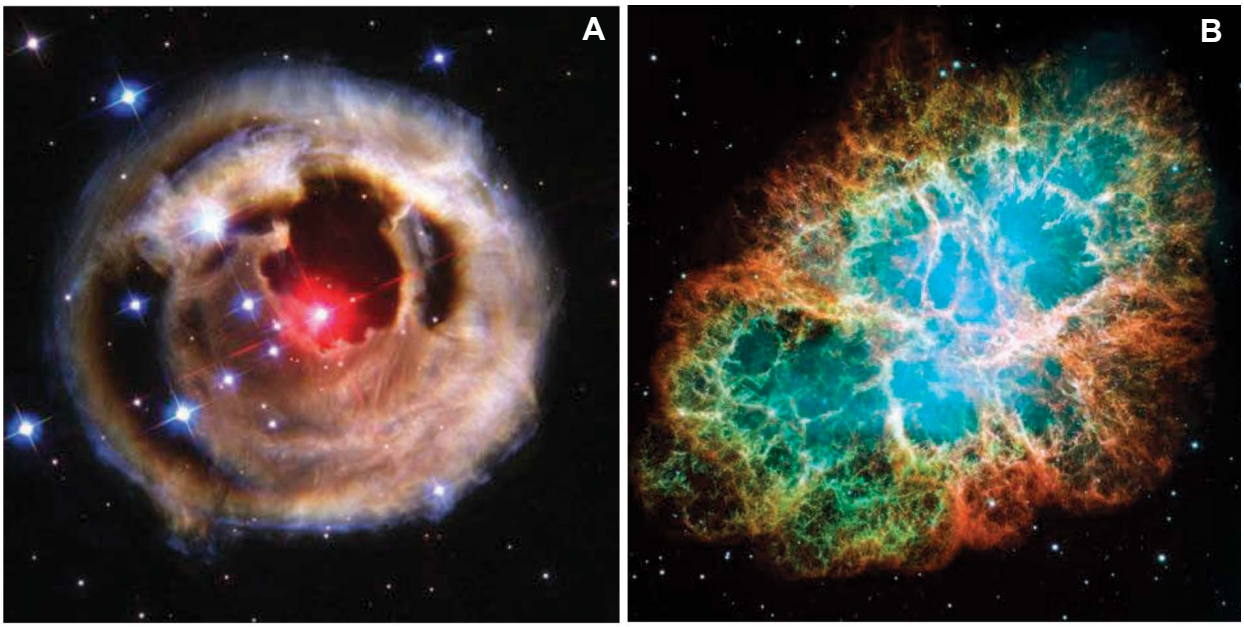

FIGURE 2. Dust-forming stars. (Hubble Space Telescope images, courtesy of NASA). (**a**) Image of star V838 Monocerotis, a "planetary nebula" that formed from dust and gas surrounding an asymptotic giant branch (AGB) star. (**b**) Image of the Crab Nebula—the remnants of a supernova. (Color online.)

with atomic number greater than 30 arise primarily through neutron-capture processes in late-stage, evolved stars. Both the *s*-process and *r*-process (i.e., rapid neutron capture; see below) nucleosynthesis involve the addition of one neutron after another until a nucleus becomes unstable and undergoes β decay, thus increasing atomic number by 1. The new element captures additional neutrons and the process repeats. Owing to the ~10 min half-life of free neutrons, these neutron-capture scenarios must occur in specific stellar environments with intense neutron fluxes—conditions not met in main sequence hydrogen-burning stars. Rather, *s*-process nucleosynthesis is thought to occur primarily in the helium-burning cores of certain red giant stars, as well as in low- to intermediate-mass asymptotic giant branch stars undergoing helium burning. Neutrons, which are initially captured on iron nuclei from previous generations of stars, lead to cascades of reactions that produce most of the stable elements heavier than iron (Käppeler 1999; Johnson 2019). In particular, as an Fe nucleus becomes neutron-rich, it undergoes β decay and transforms to cobalt, the next element in the periodic table. The *s*-process continues, element by element, to Bi, with the relative abundances of resulting isotopes approximately inversely proportional to their neutron capture cross-sections (leading, for example, to the notable generation of Mo, Zr, Ru, Sr, Ba, W, and Pb). The *s*-process can thus produce diagnostic suites of trace and minor elements in AGB minerals.

• *Rapid neutron capture (r-process*). Approximately 40% of elements heavier than iron, including all uranium and thorium atoms, arise from the rapid neutron capture process. Note that in the early history of the universe, before the emergence of the multi-generation iron-rich stars that fuel the *s*-process, the *r*-process must have dominated nucleosynthesis of heavy elements (e.g., Sneden et al. 2008). The *r*-process requires remarkable neutron fluxes, corresponding to free-neutron densities as high as 10 kg/cm^3—extreme conditions that point to the environments of neutron stars. Recent observations of a gravitational wave event (designated GW170817), coupled with intense electromagnetic radiation pulses in a wide range of wavelengths from host galaxy NGC4993, suggest that the *r*-process occurs in colliding neutron binary stars—energetic events dubbed "kilonovae" (Kasen et al. 2017; Coulter et al. 2017; Ghirlanda et al. 2019). An important diagnostic marker of the *r*-process is the anomalous abundance of the most neutron-rich stable isotopes ("*r*-only isotopes," such as ^{134}Xe and ^{136}Xe) of elements heavier than iron. It is important to note that the distinctive isotopic attributes of presolar minerals have provided the first tangible evidence for the *s*-process, *r*-process, and other major nucleosynthetic mechanisms, which were long hypothesized (e.g., Burbidge et al. 1957; Cameron 1957) but not previously supported by observations (e.g., Nittler and Ciesla 2016).

• *Proton capture nucleosynthesis.* Some proton-rich isotopes are thought to form in very high-temperature environments (>10^9 Kelvins) with high proton densities, for example, during the accretion of hydrogen onto a neutron star (Bildsten 1998).

• *Cosmic-ray spallation*. Most lithium, beryllium, and boron nuclei form through the fragmentation of more massive nuclei—transformations triggered by cosmic-ray fluxes in at least three galactic environments. Intense spallation occurs during classic core-collapse supernova events (e.g., Clayton 1983), in contrast to much more gradual spallation as a consequence of exposure to the essentially isotropic galactic cosmic ray flux. A record of spallation-induced nucleosynthesis in proximity to the early active Sun is also preserved in the most ancient solar system materials (Caffee et al. 1987; Hohenberg et al. 1990; Feigelson et al. 2002; Sossi et al. 2017; Kööp et al. 2018).

An intriguing aspect of nucleosynthesis is that the average composition of the universe evolves, from the initial 9:1 hydrogen-

to-helium mixture of 13.8 billion years ago to the present state, when ~2 wt% of H + He has been converted to heavier elements (Pagel 1997; Matteucci 2003; Johnson 2019). This evolving diversity and distribution of chemical elements has had a profound effect on the cosmic evolution of minerals, as well. In particular, the wide range of observed ratios of the isotopes of C, N, O, Si, and other elements in stellar minerals reflect a parent star's starting composition overlaid by its internal nucleosynthetic processes.

An example of this effect is provided by comparing the lower metallicity AGB stars in the Magellanic Clouds (a pair of nearby dwarf galaxies in the Local Cluster), with the more metal-rich AGB stars in the Milky Way. The atmospheres of evolved stars in the Magellanic Clouds are dominated by carbon-rich dust, in contrast to Milky Way stars that are much richer in SiC. That contrast arises because all AGB stars form and dredge up carbon, but silicon content depends on their initial metallicity (Sloan et al. 2016).

On the variety of mineral-forming stars

Three contrasting types of highly evolved stars—AGB stars, Type II supernovae, and classical novae—are thought to be the primary producers of dust in the universe and to have formed the majority of the refractory phases observed as isotopically anomalous presolar grains in chondrite meteorites. Here we review these three major types of mineral-producing stars.

Most stars for most of their lifetimes do not produce minerals. Like the Sun, the majority of stars are now fusing hydrogen to form helium in their cores; these stars lie on the so-called "Main Sequence" of the Hertzsprung-Russell diagram (e.g., Karttunen and Oja 2007; Carroll and Ostlie 2017). Approximately 90% of stars visible in the night sky are in the midst of their stable hydrogen-burning phase—extended intervals during which condensed phases are unlikely to form.

For stars greater than about one-third of the Sun's mass, additional nucleosynthesis processes eventually occur after an extended period of hydrogen burning—more than 9 billion years for the Sun, but much shorter for more massive stars [e.g., an estimated ~30 million years for stars eight times the mass of the Sun (Schröder and Connon Smith 2008; Peeples and Somerville 2013)]. Subsequent synthesis of elements heavier than helium (for example, the nucleosynthesis of carbon by the triple-α process), coupled with convective overturn to bring these heavier elements to a star's surface—a phenomenon known as "dredging"—produce the conditions by which mineral-forming elements may enter a star's dynamic atmosphere and condense as refractory phases. Consequently, stellar mineralogy primarily emerges from relatively late-stage processes in the lifetimes of stars of sufficient mass.

Stars form minerals when stellar atmospheres sufficiently enriched in C, O, Si, and other mineral-forming elements expand and cool below the condensation temperatures of refractory phases. The range of environments in presumed mineral-forming stars varies significantly in several attributes, including mass, metallicity, composition, age, and the rapidity of the mineral-forming events. All of these characteristics significantly affect the production, attributes, and survival of stellar minerals and other condensates, but the two factors that most strongly influence the formation of minerals by stars are mass and metallicity. Stellar mass plays the major role in the production of elements heavier than helium. Consequently, stars with masses from slightly less than the Sun to many times the solar mass have the potential to produce minerals at some stages of their lifetimes. In general, more massive stars produce a wider range of elements by nucleosynthesis, they produce those elements more rapidly, and they are more efficient at dispersing those elements into the interstellar medium.

Superposed on the evolution of any individual star is its initial composition—the "metallicity," defined as the percent of a star's mass comprised of elements heavier than hydrogen and helium. The metallicity of distant stars is measured relative to the Sun, which had an estimated initial composition 4.5 billion years ago of ~71 wt% hydrogen, ~27.5 wt% helium, and ~1.5 wt% "metal" (e.g., Johnson 2019). The earliest stars in the cosmos, represented by an ancient group of "Population III stars" (Tominga et al. 2007), formed from the abundant hydrogen and helium characteristic of Big Bang Nucleosynthesis and thus began their lives with metallicities less than a millionth that of the Sun—i.e., with essentially no mineral-forming elements (Frebel et al. 2009). Other stars that formed subsequently from the debris of earlier stellar generations display a range of metallicities, from significantly less than the Sun to more than twice the solar abundance of elements heavier than helium (Taylor 1996; Feltzing and Gonzales 2001; Peeples and Somerville 2013). As a general rule, stars with greater metallicity are more amenable to production of *s*-process elements from neutron capture by iron, and they are more likely to host mineral-like condensates in their turbulent atmospheres.

The composition of stellar atmospheres may be further complicated by significant mass transfer, both large-scale mixing from the mergers of different galactic sources (Clayton 1997, 2003; Lugaro et al. 1999; see Nittler and Dauphas 2006, and references therein) and local mixing, for example from a companion binary star of different type (e.g., Nittler et al. 2008; Zega et al. 2014a). The consequent intimate connection between astrophysics and the earliest phases of cosmic mineral evolution is a gradually emerging, intensely fascinating facet of natural condensed materials science.

Three types of stars—AGB stars, Type II supernovae, and classical novae, each representing post-hydrogen-burning stages of stellar evolution—have been implicated in the formation of most stellar minerals. It is important to note that these types of stars feature a complex and dynamic range of mineral-forming environments. Distributions of mineral-forming elements and their isotopic ratios reflect both the pressure-temperature-composition regime in which nucleosynthesis occurs and the dynamic convective (or explosive) processes that bring those elements to the cooler atmospheres where condensation can take place. These stars occur with a range of initial masses and metallicities, and they experience a succession of evolutionary phases, each of which may contribute in different ways to the inventory of stardust.

Asymptotic giant branch (AGB) stars. The largest producers of stardust are asymptotic giant branch (AGB) stars, which evolve from red giant stars between about 0.6 and 8 solar masses. AGB stars form spectacular planetary nebulas, which are a major source of mineral-rich dust in the galaxy (Fig. 2a). Planetary nebulas form when AGB stars enter a late-stage of nucleosynthesis characterized by fusion in a carbon- and oxygen-rich core, an inner shell of helium burning, and a surrounding shell of hydrogen burning. An important characteristic of AGB stars is a prolonged period of *s*-process nucleosynthesis, the mechanism by which existing nuclei capture neutrons one at a time to increase atomic mass, trigger β

decay, and generate new heavier isotopes and elements—notably Mo, Zr, Ru, Sr, Ba, W, and Pb. *S*-process nucleosynthesis thus enriches some AGB stars in idiosyncratic isotopes and trace elements.

Several significant "dredge up" episodes of convective overturn bring C- and/or O-rich core material to the surface, where these and other mineral-forming elements are introduced to the stellar atmosphere. The "first dredge-up," which occurs after the main sequence as stars are commencing their red giant phase, has a relatively minor effect on mineral-forming elements, though it adds ^{13}C, ^{15}N, and ^{17}O from the CNO cycle and thus changes the isotope values of C, N, and O significantly. The second dredge-up, which only occurs in stars greater than four times the Sun's mass, leads to increased ^{14}N relative to ^{12}C and ^{16}O.

A sequence of "third dredge-up" (TDU) episodes, during which carbon and *s*-process elements such as Mo and Zr are brought to the star's surface, occurs during the AGB phase of stars less than ~8 solar masses. The significant transfer of ^{12}C to the surface during TDU episodes may ultimately produce a star in which C/O > 1—an environment in which diamond, graphite, and/or carbide grain formation is favored. Depending on the variable and evolving ratio of C/O, which may range from C > O to O >> C, the dominant mineralogy will range from carbon allotropes and silicon carbide to oxides and silicates. As the primary producers of carbon in the universe, AGB stars are thought to be the source of most of the C-bearing presolar mineral grains. Indeed, more than 95% of presolar SiC grains are attributed to AGB stars (Daulton et al. 2003; Davis 2011).

Though not fully understood, an additional hypothesized phase of an AGB star's evolution has been called "cool bottom processing" (CBP), which is thought to occur as significant mass convects from the outer stellar envelope into hot interior regions. There, additional nuclear fusion reactions may occur before mass is returned to the surface (Nollett et al. 2003; however, see Lugaro et al. 2017). Characteristic changes ascribed to CBP may include the rapid production of short-lived ^{26}Al (which decays to ^{26}Mg) and destruction of ^{18}O, leading to a significant decrease in $^{18}O/^{16}O$. Furthermore, the significant destruction of ^{12}C by CBP may lead to C/O < 1, thus precluding carbide grain formation, while destruction of ^{15}N leads to increased $^{14}N/^{15}N$. The distinctive isotopic compositions of some SiC grains may thus require such cool bottom processing (Alexander and Nittler 1999; Zinner et al. 2006).

In addition to this complex evolutionary sequence, some "born-again" AGB stars are thought to experience a late-stage surge of helium burning that leads to a pulse of ^{13}C and other *s*-process, neutron-rich isotopes (Herwig et al. 2011; Fujiya et al. 2013). This distinctive isotopic mix matches some of the observed compositions of a scarce population of ^{13}C-rich silicon carbide grains.

Finally, enigmatic J-type carbon-rich stars (Abia and Isern 2000) are characterized by C > O and extreme enrichment in ^{13}C ($1 < ^{12}C/^{13}C < 10$, compared to solar values ~90), as well as enrichment of ^{14}N relative to ^{15}N. J stars, which contrast to the more abundant ^{12}C-rich N-type stars (also known as "C-rich AGB stars"), account for as many as 15% of carbon-rich stars (Morgan et al. 2003). Their origins are not well understood, but their unique compositions appear to be reflected in some presolar grains, for example, a distinctive population of "AB-type" silicon carbide grains (Liu et al. 2017a).

Supernovae. Most presolar mineral grains have isotopic compositions that conform to mixtures that are plausibly derived from AGB stars. However, a small fraction of anomalous grains, notably those with extreme concentrations of neutron-rich isotopes, demand alternative origin hypotheses. In particular, stars more massive than approximately 8 times the Sun are relatively short lived (<30 My; Karakas and Lattanzio 2014) and end in catastrophic core-collapse events called Type II supernovae ("SN-II", Fig. 2b). Following a short and intense period of core-collapse nucleosynthesis, including brief "neutron bursts" that may produce a suite of heavy element isotopes distinct from the *s*- or *r*-processes (Meyer et al. 2000; Rauscher et al. 2002), SN-II events eject a significant fraction of their mass into the interstellar environment, with consequent jumbling of isotopes from different stellar layers as the cooling, expanding, turbulent atmosphere produces various presolar minerals (Nittler et al. 1996, 2008; Travaglio et al. 1999; Hoppe et al. 2000). Shock waves associated with SN-II explosions have also been implicated in the formation and/or alteration of some presolar grains, notably nanodiamonds (Stroud et al. 2011). Diagnostic features of Type II supernovae include elevated $^{18}O/^{16}O$, as well as the production of a distinctive suite of isotopes, notably ^{26}Al, ^{44}Ti, and ^{49}V, which decay to stable ^{26}Mg, ^{44}Ca, and ^{49}Ti, respectively. Analyses of short-lived isotopes in supernova-derived SiC grains suggest that dust formation commences more than 2 yr after and continues for at least 10 yr following, the explosion (Liu et al. 2018).

Additional mineral condensation may occur as a consequence of Type Ia supernovae, which are an end stage for some white dwarf stars—the collapsed remnants of a main sequence star up to ~8 solar masses. White dwarf stars have exhausted their helium-burning phase, but they lack the critical mass (the Chandrasekhar limit; Chandrasekhar 1931) to trigger a core-collapse (SN-II) supernova. However, if that limit is eventually exceeded through mass transfer from a binary companion star, then collapse is accompanied by explosive hydrogen burning and rapid consumption of a significant fraction of carbon and oxygen to yield ejecta concentrated in heavier elements (Khokhlov et al. 1993; Mazzali et al. 2007). Type Ia supernova nucleosynthesis probably accounts for only a small fraction of observed presolar grains, and few if any examples have been confirmed. Nevertheless, recent investigations of ^{54}Cr-rich grains by Nittler et al. (2018a) may best be ascribed to SN-Ia origins.

Other varieties of exploding/colliding stars may also play as yet unconfirmed minor roles in the formation of stellar minerals. In addition to "kilonovae," which are colliding binary neutron stars that may facilitate abundant *r*-process nucleosynthesis (see above; Kasen et al. 2017; Coulter et al. 2017; Ghirlanda et al. 2019), "electron-capture supernovae" are another putative stellar source of presolar grains with anomalous excesses of neutron-rich ^{48}Ca, ^{50}Ti, ^{54}Cr, and ^{60}Fe (S. Jones et al. 2019a, 2019b).

Novae. A "nova" is a transient event, during which a star's brightness suddenly increases many orders of magnitude and then gradual dims over weeks or months. All novae occur in binary systems with one white dwarf star. The most common type of nova, and the one most closely tied to the creation of stardust, is the so-called "classical nova." If the white dwarf star and its companion (typically a main sequence or red giant star) are close enough, significant transfer hydrogen-rich material can occur. The white dwarf's newly accreted hydrogen atmosphere is heated to

extreme temperatures, resulting in thermonuclear ignition and runaway fusion, with the associated production of CNO-cycle isotopes ^{13}C, ^{15}N, and ^{17}O (e.g., Prialnik 2001). Expulsion of this atmosphere may be accompanied by the condensation of carbon- and oxygen-rich phases, including amorphous carbon, moissanite, oxides, and silicates (Gyngard et al. 2010a; Leitner et al. 2012a; Nittler and Ciesla 2016; Iliadis et al. 2018). Classic novae are significantly less energetic than supernovae and they produce correspondingly less ejecta. However, they make up for some of this difference in stardust production because they occur much more frequently than supernovae.

Pressure-temperature regimes of mineral-forming stars

Pressures and temperatures within stellar atmospheres (Fig. 1b) are generally coupled through adiabatic cooling during expansion, though they can be modified by extreme turbulence, with accompanying mixing and shockwave alteration. Given these complex environments, pressure-temperature ranges of the mineral-forming zones of stellar atmospheres are not always well known, though the occurrences of specific mineral species and mineral associations provide some constraints. The maximum possible temperature for formation of a stellar mineral is the >2000 K condensation temperature of diamond in a carbon-rich atmosphere, though actual formation temperatures in low-pressure stellar atmospheres are likely much lower (and evidence for stellar diamond is as yet ambiguous; Dai et al. 2002; Verchovsky et al. 2006; Stroud et al. 2011; Heck et al. 2014; Lewis et al. 2018). Soker and Harpaz (1999) documented AGB-sourced graphite grains with TiC cores, which limits both temperature ($T < 2200$ K) and pressure [$P < 7 \times 10^{-4}$ atm; see also Croat et al. (2005) for similar analyses based on ZrC and MoC inclusions]. Surveys of moissanite polytypes by Daulton and coworkers (Daulton et al. 2002, 2003) found that the lowest-temperature cubic (3*C*) form is dominant, which constrains temperature to a range from ~1500 to 1700 K.

Stellar oxide and silicate minerals form at temperatures similar to or lower than those of the observed carbon allotropes and carbides. Corundum and hibonite are the most refractory oxides, with formation temperatures estimated to exceed 1700 K (Ebel 2006 and references therein). By contrast, Zega et al. (2014a) documented the occurrence of pristine stellar oxide spinel grains that imply lower-temperature regimes, as $MgAl_2O_4$ condenses at 1161 K at 10^{-6} atm, and 1221 K at 10^{-3} atm.

A few rare nanoscale presolar grains point to significantly lower temperatures of formation. For example, Haenecour et al. (2016) describe an 80-nm-diameter iron sulfide grain as an inclusion in a presumed Type II supernova graphite (though origins in a low-metallicity AGB star could not be ruled out). Lodders (2003) estimates the highest condensation temperature for an iron sulfide to be troilite, FeS (~700 K at 10^{-4} atm). If the grain described by Haenecour et al. (2016) is a primary condensate, then it must have formed in a relatively cool regime and was subsequently transported to a much hotter region, where the graphite could precipitate around it. Sarangi and Cherchneff (2015) suggest that supernova ejecta can feature clumpiness and compositional heterogeneities that might support this scenario. However, Lodders (personal communications) suggests an equally plausible alternative scenario by which troilite formed from the "sulfurization" of a grain of presolar iron metal through secondary gas/solid reactions that occurred in reduced AGB winds (Lauretta et al. 1998).

Similarly, reports of stellar magnetite grains (estimated condensation at ~400 K at 10^{-4} atm) by Zega et al. (2015) have been explained by gradual oxidation (10^4 to 10^6 years) of primary native iron grains that condensed at much higher temperatures (Yoneda and Grossman 1995; Hong and Fegley 1998; Lodders 2003).

Formation pressures of stellar minerals are constrained in part by the observed sequence of condensation. For example, stellar graphite has not been found to incorporate moissanite (SiC) inclusions—an observation that places a lower pressure bound for carbon-rich stars, as SiC condenses before graphite only at pressures greater than 3×10^{-5} atm (Bernatowicz et al. 1996). Several observations also point to transient events that may raise local pressures to significantly greater than 10^{-3} atmospheres in some stellar environments. For example, the observed sizes of the largest AGB-derived presolar grains (>1 μm), including moissanite (Bernatowicz et al. 2006) and corundum (Takigawa et al. 2018), imply sustained exposure to regions of higher pressure, which in turn suggests that the pressure environments surrounding AGB stars are not radially symmetric. Mass outflows from such stars are likely influenced by jets and clumps, as well as by periodic shocks in the atmosphere above the photosphere. These events enhance local density and thus promote grain growth (Bernatowicz et al. 1996; Chigai et al. 2002; Gobrecht et al. 2016). In addition, stacking disorder observed for several minerals in TEM studies (Stroud et al. 2011; Zega et al. 2014a), as well as surface irregularities on otherwise subhedral crystals (Takigawa et al. 2018), could point to grain-to-grain impact-induced strain in stellar atmospheres. Finally, the shock waves of supernovae have been implicated in the formation of some presolar nanodiamonds (Stroud et al. 2011), as well as the possible transformation of $MgSiO_3$ enstatite to the high-pressure bridgmanite polymorph (Vollmer et al. 2007).

The application of cluster analysis to stellar minerals

A central theme of the evolutionary approach to mineral classification is that many IMA mineral species emerge multiple times during the evolution of stars, planets, and moons. Each new paragenetic process is likely to impart a distinctive suite of attributes to minerals as they form; therefore, we classify each unique combination of mineral species and paragenetic mode as a distinct natural kind.

Two types of information contribute to the recognition of mineral natural kinds. In the proposed evolutionary system of mineralogy, we link mineral species to distinctive mineral-forming environments—major paragenetic modes. Thus, moissanite formed in the explosive regime of a Type II supernova ("*SN-II moissanite*") is different from moissanite formed in the evolving atmosphere of an AGB star ("*AGB moissanite*") or in a classic nova explosion ("*CN moissanite*"). Additional mineral-forming stellar environments may be confidently documented in the future, at which time the classification system could easily be expanded.

Extending this approach, the opportunity exists to further subdivide minerals based on distinctive combinations or "clusters" of attributes, including trace and minor elements, isotopic ratios, solid and fluid inclusions, grain size and morphology, structural defects, and other diagnostic characteristics. Tabulations of attributes of analyzed mineral specimens, for example the Presolar Grain Database that now incorporates information

on ~20 000 moissanite grains (Hynes and Gyngard 2009; see https://presolar.physics.wustl.edu/ accessed 24 Jan 2019), present the opportunity to examine clusters of minerals based on multiple attributes in ever greater detail. Thus, for example, stellar moissanite grains have been subdivided into as many as 12 groups based primarily on ranges of Si and C isotopes (e.g., Davis 2011; Zinner 2014). Several of these groups are ascribed to AGB stars of differing mass, metallicity, and/or age—aspects of a star that are reflected in evolving element and isotope ratios. Cluster analysis thus has the potential to reveal a range of SiC subsets that have implication for understanding stellar evolution (Boyd 1991, 1999; Bailey 1994; Millikan 1999; Everitt 2011; Hazen 2019). However, for the purposes of this evolutionary system of mineralogy, origins in the atmosphere of an AGB star—whatever the mass, metallicity, or dredge-up stage—is considered to be one paragenetic mode. Similarly, stardust formation through Type II supernovae explosions, in spite of varied shells and stages of mineral formation in the evolving object, is also treated as one paragenetic mode.

Systematic evolutionary mineralogy: Part I—Stellar mineralogy

At least 24 different crystalline and three amorphous condensed phases, associated with 41 natural kinds, have been identified as stellar minerals (e.g., Lodders and Amari 2005; Davis 2011; Zinner 2014), as detailed in Table 1. The following section summarizes stellar mineralogy based on stardust analyzed since the first discoveries of 1987 (Lewis et al. 1987; Bernatowicz et al. 1987; Zinner et al. 1987) and lists all confirmed or likely species of stellar minerals of which we are aware as of 10 October 2019. Table 1 also lists 14 as yet unconfirmed stellar minerals, including native elements, nitrides, silicides, phosphides, and oxides, that have been reported as nanoscale inclusions but have not yet been fully described or independently confirmed.

This field is evolving rapidly, both in terms of the variety of stellar mineral species identified and the ranges of distinctive chemical and physical properties displayed by those minerals. For example, Lodders and Amari (2005; their Table 9) catalog more than 30 IMA-approved mineral species that might occur in stellar atmospheres on the basis of thermodynamic equilibrium condensation sequences of the most refractory phases of 17 cosmically abundant elements, including Na, Mn, Ni, P, Cl, and K, for which no stellar condensed phases have yet been confirmed. Consequently, we expect that the list of condensed phases known to form in the atmospheres of stars will expand significantly in the coming years.

A note regarding nomenclature

Minerals are arranged first by chemical class (i.e., Native Elements; Sulfides; Oxides; etc.), as employed in the revolutionary third edition of James Dwight Dana's *System of Mineralogy* (J.D. Dana 1850; see also Hazen 1984) and subsequently widely adopted and expanded (e.g., Edward S. Dana and Ford 1947; James D. Dana et al. 1973; Gaines et al. 1997). Secondary headings indicate IMA-approved mineral species (i.e., "diamond" or "corundum") or, in the case of non-crystalline phases, an appropriate compositional name (e.g., "amorphous Al_2O_3" or "silicate glass").

The evolutionary system of mineralogy emphasizes paragenetic modes of minerals in addition to their chemical compositions and atomic structures. Therefore, we adopt a binomial nomenclature for each suspected natural kind of mineral in stardust (e.g., "SN-II diamond" or "AGB chromite"). The case of stellar mineralogy is especially revealing in this regard. All minerals formed in stellar environments are characterized by significantly non-solar major and trace isotopic compositions—attributes that clearly differentiate these minerals from their terrestrial or solar nebular counterparts. The sometimes extreme isotopic deviations from solar averages, as well as idiosyncratic suites of trace and minor elements, often point to a specific type of host star. Such diagnostic element and isotope signatures suggest that presolar minerals, though often examples of relatively common terrestrial mineral species, represent distinctively non-terrestrial natural kinds.

An added complexity when dealing with stardust mineralogy is the occurrence of compositionally homogeneous domains, subgrains, or inclusions only a few nanometers in diameter that are encased in larger mineral grains. For example, it is difficult to know whether reports of isolated concentrations of Fe-Ni-Si atoms (Hynes 2010) constitute valid condensed silicide phases. In instances where such localized chemical concentrations have been observed, but no diagnostic electron diffraction or other structural information has been obtained, we record "Other possible phases" under the appropriate compositional group.

Native Elements

Allotropes of carbon, including diamond, graphite, and varieties of non-crystalline C, are abundant presolar phases (Davis 2011). These and other carbon-bearing phases were among the earliest stellar minerals to be recognized, both because of their extreme isotopic anomalies and their relative ease of concentration through acid dissolution.

At least three forms of iron, alloyed variously with Ni, Ru, Os, and other metallic elements, have been confirmed as "refractory metal nuggets," which occur as inclusions in stellar graphite (Croat et al. 2003, 2008, 2013; Hynes et al. 2010). In some alloys Ni or Ru may be locally greater than Fe. In addition, nano-inclusions of native Os with minor Mo, Ru, and Fe have been reported as inclusions in SN-II graphite (Croat et al. 2005, 2013).

Diamond (C). Diamond was suggested by Hazen et al. (2008) to be the first mineral in the cosmos, presumably formed by vapor deposition as the carbon-bearing atmospheres of highly evolved stars expanded and cooled significantly below the 4400 K maximum condensation temperature of diamond. In parallel to that idea, diamond was the first presolar mineral to be positively identified (Lewis et al. 1987), and it remains the most abundant known presolar phase, both in terms of wt% (~1400 ppm in CM chondrites) and numbers of grains (Davis 2011). Based on microstructural studies, for example by Daulton et al. (1996), the source of these nanodiamonds is likely vapor deposition. However, in spite of these discoveries, an ancient stellar (as opposed to solar nebular) source for meteoritic presolar nanodiamonds has not been unambiguously verified (Nuth and Allen 1992; Ozima and Mochizuki 1993; Richter et al. 1998; Dai et al. 2002; Stroud et al. 2011). In the words of Zinner (2014), "Although diamond is the most abundant presolar grain species (~1400 ppm), … it remains the least understood."

The principal difficulty in characterizing presolar diamond has been their diminutive size, typically less than 10 nm diameter,

with an average size of 2 to 3 nm diameter, corresponding to fewer than 2000 carbon atoms. As a result, most analytical studies have of necessity measured average compositions of millions of grains—averages that, in general, do not deviate significantly from the observed solar $^{12}C/^{13}C \sim 90$ or $^{14}N/^{15}N \sim 249$ (Russell et al. 1991, 1996; Daulton et al. 1996; Dai et al. 2002). [Note that throughout this contribution we use the somewhat quirky isotope ratio conventions employed in most astromineralogy publications; namely, $^{12}C/^{13}C$, $^{14}N/^{15}N$, $^{17}O/^{16}O$, $^{18}O/^{16}O$, $^{29}Si/^{28}Si$, and $^{30}Si/^{28}Si$ (as opposed, for example, to δ notation), because of the extreme deviations from solar averages (e.g., Davis 2011; Zinner 2014).] Until recently it has been impossible to characterize individual diamond grains that might bear the distinctive isotopic signatures of stars (Heck et al. 2014; Lewis et al. 2018).

Two studies point to plausible stellar sources for some presolar diamonds. Verchovsky et al. (2006) successfully isolated a slightly larger size fraction of crystallites—the largest 1% of grains that collectively yield isotopically light carbon, heavy nitrogen, and noble gas signatures characteristic of some AGB stars. However, Stroud et al. (2011) found the co-occurrence of a "glassy carbon" fraction in these residues, calling into question whether the AGB isotopic anomalies are associated with diamond, the amorphous phase, or both.

Additional evidence for populations of stellar diamonds comes from Lewis et al. (2018), who employed NanoSIMS with a minimized high-resolution 50 nm beam diameter to examine tens of thousands of discrete small volumes, each with approximately 1000 nanodiamonds per observation. They suggest that if stellar diamonds with large isotopic anomalies are present in the sample, then the Gaussian statistical distribution of observed $^{12}C/^{13}C$ should display a significant broadening compared to similar measurements on a homogeneous diamond population. Lewis and coworkers found that the average carbon isotopic value was close to solar, in agreement with prior studies, but they also documented significant broadening, which they attributed to multiple isotopic values, including both ^{13}C-enriched and depleted grains, presumably from multiple stellar sources. Nevertheless, the likely occurrence of amorphous carbon in all diamond residues (Stroud et al. 2011) makes unambiguous recognition of stellar diamond problematic.

With these uncertainties in mind, we provisionally list two kinds of stellar diamond:

AGB diamond. Nanometer-scale diamond with isotopically light carbon (e.g., high $^{12}C/^{13}C$), heavy nitrogen (low $^{14}N/^{15}N$), and noble gas signatures characteristic of AGB stars (Verchovsky et al. 2006; Lewis et al. 2018).

SN-II diamond: Nanometer-scale diamond with low $^{12}C/^{13}C$, possibly associated with isotopically anomalous xenon isotopes (Lewis et al. 1987; Clayton et al. 1995; Lewis et al. 2018).

Graphite (C). Grains of stellar graphite were among the first presolar minerals to be discovered, initially based on anomalous neon isotopes (Amari et al. 1990), and they have received intense subsequent study (Amari et al. 1994, 1995a, 1995b, 2004; Bernatowicz et al. 1996, 2006; Croat et al. 2003, 2005, 2008; Stadermann et al. 2005; Davis 2011; Groopman et al. 2012; Zinner 2014 and references therein; Groopman and Nittler 2018). Presolar graphite constitutes ~10 ppm by weight of CM chondrite meteorites, with sizes up to 20 μm in diameter (Zinner et al. 1995). The relative abundance of stellar graphite is reflected in the Presolar Grain Database, which records 2200 analyzed grains (Hynes and Gyngard 2009; see https://presolar.physics.wustl.edu/ accessed 24 Jan 2019).

The morphologies of stellar graphite grains are varied, with one distinctive population of grains having cores of randomly oriented graphene sheets surrounded by well-graphitized "onion-like" concentric layers (Fraundorf and Wackenhut 2002; Zinner 2014; Fig. 3a). Other "cauliflower" type grains, by contrast, form as aggregates of smaller crystallites (Bernatowicz et al. 1996; Hoppe et al. 1995; Fig. 3b). Most of these stellar graphite grains have been extracted from the widely available Murchison and Orgueil carbonaceous meteorites. These samples have been further divided into density fractions—aliquots that reveal intriguing differences in size and isotopic attributes of two populations described as higher density (HD) and lower density (LD). The carbon isotope ratios of stellar graphite vary widely: $2 < {}^{12}C/^{13}C < 7500$ (Hynes and Gyngard 2009), with most grains isotopically lighter than the solar average of ~90. Furthermore, the HD fraction of grains is on average smaller and of greater $^{12}C/^{13}C$ than the LD fraction. Identification of different stellar origins depends additionally on isotopic ratios of minor O, N, and Si impurities, as well as trace amounts of diagnostic *r*-process and *s*-process elements. We list three types of stellar graphite, originating in three contrasting stellar environments, as distinguished by their chemical and isotopic anomalies, coupled with their physical properties and morphologies (e.g., Davis 2011; Zinner 2014).

AGB graphite: Approximately 30% of stellar graphite grains, the great majority of which are from the higher density (HD) population, have high $^{12}C/^{13}C$ relative to solar abundances and display enrichment in characteristic *s*-process elements Zr, Mo, and Ti, which form carbide inclusions up to 200 nm in diameter (Amari et al. 1994, 1995b, 1995c, 2006; Bernatowicz et al. 1996; Croat et al. 2005; Heck et al. 2009a; Meier et al. 2012). AGB graphite grains typically display platy or onion-like morphologies and are, on average, smaller than other kinds (Croat et al. 2008). They display a range of crystallinity, as revealed by electron microscopy (Bernatowicz et al. 2006) and Raman spectroscopy (Wopenka et al. 2011a).

A small fraction of AGB graphite grains display extremely low $^{12}C/^{13}C$ values relative to solar, coupled with Ca and Ti isotopic anomalies. The most likely sources are enigmatic carbon-rich born-again AGB stars, or J stars (Jadhav et al. 2008, 2013; Nittler and Ciesla 2016). We suggest that the paragenetic mode of these grains is the same as that of other AGB star grains, i.e., gradual condensation from the gas phase. However, cluster analysis may demonstrate that these grains point to the existence of multiple varieties of AGB graphite.

SN-II graphite: An estimated 60% of stellar graphite grains, including the majority of LD population grains (Zinner et al. 2006), display compositional characteristics of Type II supernovae, with low $^{14}N/^{15}N$, high $^{18}O/^{16}O$, and remnants of ^{26}Mg, ^{44}Ca, ^{49}Ti, and other diagnostic trace isotopes (Nittler et al. 1996; Stadermann et al. 2005; Jadhav et al. 2013; Zinner 2014, and references therein). These grains are typically irregularly crystallized with "cauliflower" morphology, often with TiC cores and sometimes numerous (up to hundreds) of TiC inclusions from 30 to 230 nm in diameter (Amari et al. 1995b; Soker and Harpaz 1999; Croat et al. 2008), as well as distinctive inclusions of Fe-Ni metal and/or

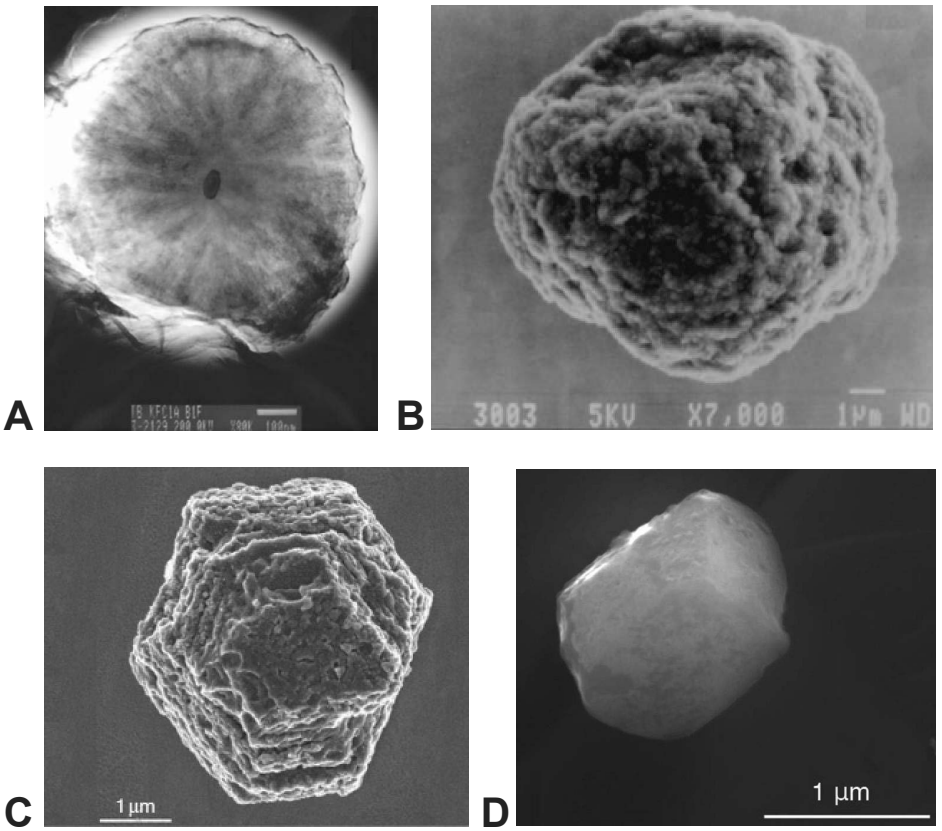

FIGURE 3. Electron microscope images of stellar minerals. (**a**) Cross section of a 1 μm diameter "onion" AGB graphite with central khamrabaevite (TiC) inclusion (Zinner 2014); (**b**) 13 μm diameter "cauliflower" SN-II graphite grain—a composite of smaller crystallites (Zinner 2014); (**c**) 4.5 μm diameter euhedral "mainstream" AGB moissanite (SiC) crystal (Zinner 2014); (**d**) 1.4 μm diameter euhedral AGB corundum (Al_2O_3) crystal (Takigawa et al. 2018).

Os-rich regions (Stadermann et al. 2005; Groopman et al. 2012).

CNova graphite: A small population of graphite grains has very low $^{12}C/^{13}C$ (<10) and high $^{30}Si/^{28}Si$, as well as neon isotope anomalies, which collectively point to a possible origin in classical novae (Amari et al. 2001c; Jadhav et al. 2008; Heck et al. 2009a; Haenecour et al. 2016). Cluster analysis of stellar graphite grains (in progress) may clarify the extent to which these samples represent a discrete population with a different paragenetic mode.

Amorphous carbon (C). A low-density fraction of presolar carbon occurs in amorphous and/or structurally disordered states, possibly representing several distinct types of non-crystalline C. For example, Stroud et al. (2011) report disordered "glassy" carbon with *sp*2 bonding—a population of grains that displays distinctive Raman spectra (Wopenka et al. 2011b). However, until more definitive structural and compositional information is available, we catalog only one kind of amorphous carbon.

Stellar amorphous C: Non-crystalline carbon with anomalous $^{12}C/^{13}C$.

Refractory metal nuggets (Fe, Ni, Ru, Cr, Mo, Os, Ir). Refractory metal alloys, incorporating two or more of Fe, Ni, Ru, Cr, Mo, and Os, represent intriguing minor phases in stardust. At least three different groups of Fe-bearing alloys have been identified as inclusions in SN-II graphite (Bernatowicz et al. 1996; Croat et al. 2003, 2005, 2008, 2010, 2013; Stadermann et al. 2005; Gyngard et al. 2018). Croat et al. (2003, 2005, 2008) and Hynes (2010) characterized both native iron (the α-iron alloy of Fe:Ni, sometimes referred to as "kamacite"; space group *Im*3*m*) and taenite (the γ-iron alloy of Fe-Ni; space group *Fm*3*m*) by ion probe and electron microscopy. In addition, Fe combines with Ni, Ru, Os, and Mo in metal inclusions in graphite, presumably in space group $P6_3/mmc$ (Croat et al. 2008; Rubin and Ma 2017).

The variable compositions of stellar iron alloys present a classification challenge. Consider the case of the Fe-Ni alloy taenite, which is observed to vary from Fe >> Ni to Ni > Fe in a continuous solid solution. IMA protocols would assign different mineral names to the iron- and nickel-rich end-members of this solid solution. However, in the evolutionary system of mineralogy, we lump all members of a continuous solid solution that form under similar conditions as a single natural kind. Thus, even though Ni may approach 60 atom % in some taenite inclusions (thus approximating in composition the IMA-approved mineral species awaruite), we lump all of these inclusions into *SN-II taenite*.

The case of the $P6_3/mmc$ alloy of Fe-Ni-Mo-Cr-W-Ru-Os-Ir is more difficult to resolve. These nano-inclusions in graphite, which may represent the earliest condensates in some C-rich stars, display extensive solid solutions, with some individual inclusions dominated by Fe, Ru, or Os. Croat et al. (2013) point to immiscible regions, for example, between Fe-Ni-rich and Ru-

rich compositions. The case of osmium, with ~50-nm inclusions with Os >70 atom %, would seem to demand that native Os be considered a valid stellar mineral. The case of ruthenium is less clear-cut. Most grains have Fe >> Ru, but a few grains have Ru > Fe (up to $Ru_{77}Fe_{23}$), suggesting an extensive Fe-Ru solid solution, but with a possible immiscibility region (Croat et al. 2013). Given that uncertainty, we include native ruthenium as a stellar mineral. However, if additional data on the compositional range of metallic inclusions in SN-II graphite reveal a continuous solid solution among Fe, Ni, Ru, Os, and other elements, then we may in the future ascribe most or all of these "refractory metal nuggets" to a single natural kind.

SN-II iron: The α-iron alloy [(Fe,Ni); space group *Im*3*m*], sometimes called "kamacite," occurs both as isolated inclusions and epitaxially attached to TiC inclusions in SN-II graphite (Croat et al. 2003). These Fe-rich grains, extracted from the Murchison meteorite, contain 0 to 24 atom % Ni.

SN-II taenite: Taenite [(Fe,Ni), space group *Fm*3*m*] occurs as nano-inclusions attached through epitaxial growth to TiC inclusions in SN-II graphite from the Murchison meteorite (Croat et al. 2003). The majority of grains have Fe > Ni, though a few grains have up to 60 atom % Ni.

SN-II ruthenium: Croat et al. (2005) describe nano-inclusions (>20 nm diameter) of Fe-Ru alloys in SN-II graphite, mostly with Fe > Ru, but some of which have Ru >> Fe (ranging to as high as $Ru_{77}Fe_{23}$). In addition, Croat et al. (2013) report a 21-nanometer-diameter Ru-dominant refractory metal inclusion of composition ($Ru_{29}Mo_{24}Fe_{17}Os_{13}Ir_{13}$ $Ni_2W_1Cr_1$)—a composition that underscores the difficulty of ascribing many such nuggets to a single element end-member. Note that the hexagonal unit-cell dimensions of this grain (a = 2.80 Å; c = 4.44 Å) are consistent with the $P6_3/mmc$ space group of native ruthenium.

SN-II osmium: Croat et al. (2005) report a single 50-nm-diameter Os-rich inclusion ($Os_{79}Mo_{10}Ru_9Fe_2$) in a SN-II graphite grain. Croat et al. (2013) describe a grain of similar composition ($Os_{74}Ru_9W_6Mo_4Fe_3Ir_2$), with hexagonal symmetry (a = 2.77 Å; c = 4.48 Å), consistent with the $P6_3/mmc$ space group of elemental osmium. These unusual grains do not fall close to the Fe-Ni-Ru composition space of many other stellar alloy inclusions; therefore, we recognize osmium as a distinct stellar mineral. The sequence of Os condensing prior to its inclusion in graphite points to the formation in a supernova environment.

Carbides

Grains of stellar carbides, primarily moissanite (SiC) but also khamrabaevite (TiC) in some cases significantly enriched in V, Mo, Zr, and/or Ru, are among the most abundant and well-studied presolar grains (Davidson et al. 2014; Zinner 2014). Almost all carbide grains found in meteorites are thought to arise from condensation in stellar atmospheres, in contrast, for example, to oxides and silicates, most of which bear the solar system's isotopic ratios and are thus thought to be condensates from the solar nebula. The majority of these isotopically anomalous carbide phases form in the chemically reduced atmospheres of carbon-rich AGB stars.

Moissanite (SiC). Interstellar silicon carbide was first recognized as a component of stars from distinctive IR emission spectra of the dust-rich atmosphere of carbon stars (Treffers and Cohen 1974; Forrest et al. 1975). Subsequent discovery of isotopically anomalous moissanite grains in the insoluble residues of CM meteorites (Zinner et al. 1987; Lewis et al. 1990, 1994) established SiC as the second known stardust mineral. Moissanite, though less abundant than presumed presolar diamonds, averages ~30 ppm in CM chondrites (Davis 2011; Davidson et al. 2014), with reported concentrations as high as 160 ppm in some meteorites (Leitner et al. 2012b; see Zinner 2014).

Moissanite forms the largest known stellar mineral grains, with some crystals greater than 20 μm in diameter (Gyngard et al. 2018), though most grains are less than a micrometer in diameter (Zinner et al. 2007; Gyngard et al. 2009; Heck et al. 2009b; Hoppe et al. 2010; Davis 2011; Fig. 3c). Consequently, SiC has received the most detailed study of any stellar mineral, with more than 17300 measured grains recorded in the Presolar Grain Database (Hynes and Gyngard 2009; see https://presolar.physics.wustl.edu/ accessed 24 Jan 2019).

The isotopic ratios of carbon, silicon, and nitrogen (the latter a ubiquitous impurity in stellar SiC), as well as varied concentrations of trace elements and isotopes of characteristic *s*-process elements (e.g., Ti, Zr, and Mo) and extinct radionuclides (notably short-lived ^{26}Al, ^{44}Ti, and ^{49}V recognized by their decay products ^{26}Mg, ^{44}Ca, and ^{49}Ti), have been used to differentiate moissanite into as many as seven varieties (Davis 2011), representing both AGB stars and explosive environments of novae and supernovae (Table 1; Fig. 4). In addition, rare anomalous individual grains point to additional possible origins or evolutionary pathways for moissanite grains in stellar atmospheres that are not yet fully understood (Leitner et al. 2012b; Nguyen et al. 2016). This diversity reflects not only the stability of SiC in various carbon-rich stellar environments, but also the benefits (and complexities) arising from broad surveys of large numbers of presolar grains.

It should be noted that an evolving nomenclature for types of stellar moissanite has already gained some traction in the astromineralogy community. Approximately 9 in 10 stellar SiC grains bear the distinctive isotopic signatures of AGB stars—characteristics of so-called "mainstream" stellar SiC (e.g., Zinner 2014). The first SiC grain to be discovered with a markedly different isotopic composition, presumably formed in a Type II supernova, was called "Type X" (Amari et al. 1992; Nittler et al. 1996; Hoppe et al. 2000). Subsequent distinctive finds of presolar SiC were called types Y and Z (Alexander 1993; Hoppe et al. 1994, 1997; Amari et al. 2001a; Nittler and Alexander 2003), followed by A, B, and C. Types A and B were later merged into "Type AB," though Liu et al. (2017c) subsequently proposed a split into AB1 and AB2 based on nitrogen isotopes. In addition, Liu et al. (2016) suggested splitting C into C1 and C2 based on carbon isotopes, while Type X is sometimes subdivided into X0, X1, and X2 (Lin et al. 2010). It is not yet possible to unambiguously assign every stellar SiC grain to one category, much less to one stellar paragenesis.

In this study, we recognize three major paragenetic processes that produce the great majority of stellar moissanite—AGB stars, Type II supernovae, and classical novae. In addition, cluster analysis studies of presolar SiC grains are now in progress to provide a quantitative basis for distinct subdivisions of stellar moissanite.

An important characteristic of moissanite is its diverse array of stacking polytypes, of which more than 200 have been documented in synthetic samples (Kelly et al. 2005; Cheung 2006). Presolar moissanite grains are found in two principal structural polytypes,

most commonly in the lowest-temperature cubic (3*C*) form, with a smaller fraction of the hexagonal (2*H*) polytype (Daulton et al. 2002, 2003; Bernatowicz et al. 1987, 2003; Alexander et al. 1990; Amari et al. 1990, 1994, 2001a, 2001b, 2001c; Liu et al. 2017b), though a few grains with higher-order polytypes have been reported (Liu et al. 2017b; Gyngard et al. 2018).

Hints regarding the pressure of formation of stellar moissanite are provided by the absence of SiC inclusions in graphite, indicating that graphite precipitates first. Such a condensation sequence requires that pressures in the stellar atmosphere are less than 3×10^{-5} (Bernatowicz et al. 1996), at which pressure the condensation temperature of SiC falls significantly below 2000 K.

As with presolar graphite, some moissanite grains incorporate inclusions of other refractory phases, including rare examples of graphite, Ti(N,C), (Mg,Al)N, and Fe-Ni metal (Zinner 2014; Gyngard et al. 2018).

AGB moissanite: Representing ~90% of all stellar SiC grains, mainstream AGB moissanite is characterized by the distinctive combination of low $^{12}C/^{13}C$, high $^{14}N/^{15}N$, and abundant *s*-process trace elements, including Ti, Zr, and Mo (Nittler et al. 1996). Unlike polycrystalline SiC from Type II supernovae, AGB moissanite grains are typically single crystals (Stroud et al. 2004a; Hynes et al. 2010). Several authors suggest that the distinctive isotopic signatures of these abundant SiC stellar grains point to mixing of several galactic sources (Clayton 1997, 2003; Alexander and Nittler 1999; Lugaro et al. 1999).

Several moissanite grains (a few percent of presolar SiC), dubbed "Y" type, are presumed to come from AGB stars with ~50% solar metallicity (Hoppe et al. 1994). These grains have the unusual combination of high $^{12}C/^{13}C$ and high $^{14}N/^{15}N$ (Amari et al. 2001a; Nguyen et al. 2018), possibly with excesses of *s*-process Ti and Mo isotopes (Larry Nittler, personal communications). In addition, a few percent of stellar SiC grains, called "Z" grains, are ascribed to AGB stars with ~25% solar metallicity and have low $^{12}C/^{13}C$, high $^{14}N/^{15}N$, low $^{29}Si/^{28}Si$, and high $^{30}Si/^{28}Si$, in combination with excess *s*-process ^{50}Ti and ^{96}Mo. These attributes are thought to indicate low-mass stars with low metallicity (Hoppe et al. 1997; Nguyen et al. 2018). Note that a continuum may exist from Z- to Y- to mainstream-type AGB moissanite; further investigation by cluster analysis is thus warranted.

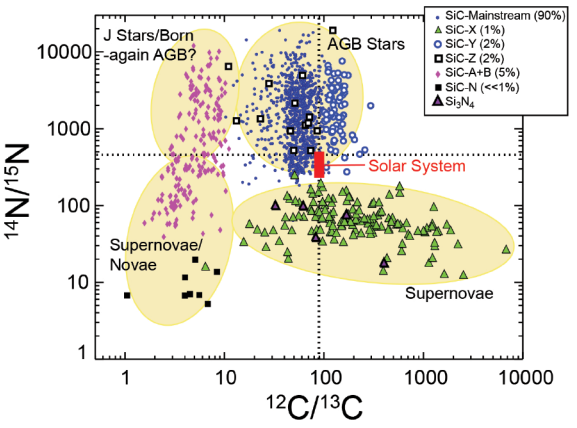

FIGURE 4. Isotope ratios for carbon and nitrogen in presolar moissanite (SiC) and nierite (Si_3N_4) reveal clustering that corresponds to several distinct natural kinds of stellar minerals, formed near different kinds of stars. Courtesy of Zinner (2014). Future multi-dimensional cluster analysis and visualization of these data coupled with Si isotopic and trace element measurements have the potential to reveal more definitive differentiations of the natural kinds of stellar SiC. (Color online.)

Additional subtypes of moissanite can be confidently ascribed to origins through condensation in the atmosphere of a late-stage AGB star. So-called "AB-type" moissanite is characterized by the distinctive combination of very low $^{12}C/^{13}C$ (<10) and a wide range of $^{14}N/^{15}N$ (from significantly greater to significantly less than solar), without significant enrichment in *s*-process trace elements—attributes that point to a carbon-rich J star or born-again AGB star (Hoppe et al. 1995; Huss et al. 1997; Amari et al. 2001b; Nittler and Alexander 2003; Liu et al. 2017a, 2017c; Nguyen et al. 2018). Indeed, cluster analysis of these grains may reveal two distinct sources (Amari et al. 2001b), with born-again AGB grains characterized by anomalous ^{32}S, a byproduct of ^{32}Si decay (Fujiya et al. 2013). Note that Liu et al. (2017c) suggest that AB moissanite should be divided into two subgroups—those with $^{14}N/^{15}N$ < solar (proposed to derive from Type II supernovae) and those with $^{14}N/^{15}N$ > solar (probably from J stars).

SN-II moissanite: Two distinct populations of stellar SiC, most of which are aggregates of nanocrystals (a consequence of relatively rapid crystallization), have been ascribed to different Type II supernova processes. C-type moissanite, representing only about one in a thousand stellar SiC grains, is characterized by low $^{14}N/^{15}N$, as well as significant excesses of ^{29}Si and ^{30}Si relative to ^{28}Si (Amari et al. 1999; Croat et al. 2010). Significant ^{26}Mg and ^{44}Ca reveal the production of short-lived radioactive ^{26}Al and ^{44}Ti (Gyngard et al. 2010b). Note that Liu et al. (2016) further divided C moissanite into C1 and C2 types, based on differences in $^{12}C/^{13}C$.

Fewer than 2% of stellar moissanite grains have been identified as "X"-type, with diagnostic isotopic signatures of Type II supernovae. All X-type silicon carbide grains display low $^{14}N/^{15}N$, $^{29}Si/^{28}Si$, and $^{30}Si/^{28}Si$, and significant ^{26}Mg, ^{44}Ca, and ^{49}Ti (Liu et al. 2018). Grains of X moissanite are also distinguished by their polycrystalline habit, with crystallites typically from 10 to 200 nm diameter.

Note that Lin et al. (2010) subdivide these grains into three distinct groups; the division of X0, X1, and X2 moissanite is based primarily on $^{29}Si/^{30}Si$, with high, average, and low values relative to solar average, respectively. However, Zinner (2014) lumps all X-type moissanite grains into a single group, and it seems plausible that cluster analysis of "X"-type SiC grains will reveal a continuum among these grains rather than three distinct natural kinds. Consequently, we group all X-type moissanite grains together and suggest that cluster analysis of X-type stellar SiC is warranted.

CNova moissanite: Approximately one in a thousand moissanite grains have very low $^{12}C/^{13}C$ and $^{14}N/^{15}N$, very high $^{30}Si/^{28}Si$, and neon isotope anomalies that point to possible origins in classical novae (Amari et al. 2001c; José and Hernandez 2007; Liu et al. 2016)—characteristics that match those of nova graphite. Note that these grains have also been designated "putative nova grains" or "PNG" moissanite. Further studies employing cluster analysis will help to resolve whether these grains represent a population characterized by a distinct paragenetic mode.

Khamrabaevite (TiC). Nanograins of titanium carbide up to 200 nm in diameter have been found in the cores and as inclusions in many presolar graphite grains (Fig. 3a; Soker and Harpaz 1999; Croat et al. 2005, 2011; Stadermann et al. 2005; Bernatowicz et al. 2006; Groopman et al. 2012). Most of these grains appear to predate graphite formation, having been swept up during graphite crystallization and, in some instances serving as nucleation sites for graphite.

AGB khamrabaevite: TiC subgrains in AGB graphite are typically enriched in *s*-process elements, including V, Zr, Mo, and Ru. Presolar graphite grains with internal TiC seeds constrain both 1.0 < C/O < 1.2 and formation conditions ($P < 7 \times 10^{-4}$ atm) (Soker and Harpaz 1999).

SN-II khamrabaevite: Titanium carbide nano-crystals are common in the cores of SN-II graphite grains. These TiC grains often display significant V for Ti substitution, but not substitution by Zr, Ru, or Mo, which arise from the *s*-process in AGB stars (Croat et al. 2003, 2011; Groopman et al. 2012).

AGB (Mo,Zr)C: Bernatowicz et al. (1996) report various carbide inclusions in AGB graphite, most commonly TiC but also Ti-Mo-Zr carbides, some of which are nearly pure (Mo,Zr)C. Bernatowicz et al. (1996) suggest a crystallization sequence upon cooling of ZrC first (at $T \sim 1800$ K), followed by MoC and TiC. Note that neither molybdenum nor zirconium carbides are yet IMA-approved mineral species.

Cohenite (Fe_3C). Bernatowicz et al. (1999) reported grains of the iron carbide cohenite (with orthorhombic symmetry) as inclusions in a SN-II graphite.

SN-II cohenite: Nanograins as inclusions in SN-II graphite.

SN iron carbide [$(Fe,Cr)_7C_3$]: Croat et al. (2005) report a single grain of hexagonal iron carbide [metal composition ($Fe_{73}Cr_{21}Ti_6$)] as an inclusion in an "onion" AGB graphite. The hexagonal unit-cell parameters, $a = 6.95$ Å and $c = 4.5$ Å, match a known synthetic phase (Fe_7C_3; space group $P6_3/mc$). Note that this iron carbide is not yet an IMA-approved mineral species.

Other possible stellar carbides. Some stellar TiC grains display local concentrations of Mo, Zr, and Ru-rich carbides (Bernatowicz et al. 1996; Croat et al. 2008), though these regions are not obviously separate inclusions of distinct phases. Similarly, Croat et al. (2011) describe Al-rich regions in TiC subgrains in SN-II graphite; they suggest that cubic ($a = 4.2$ Å) Ti_3AlC might be present.

Silicides [Unconfirmed]. A wide variety of nanoscale inclusions, subgrains, and/or local element concentrations have been reported in stellar moissanite and graphite. While it is not yet proven that these compositional regions are discrete mineral phases, potential stellar minerals include two iron-nickel silicides, possibly $(Fe,Ni)_2Si$, and/or $(Fe,Ni)_3Si$, as inclusions in SN-II (X-type) moissanite (Hynes 2010; Hynes et al. 2010). Neither the composition nor structure type was determined; therefore, stellar silicide is listed here as an unconfirmed astromineral.

Phosphides [Unconfirmed]. Lodders and Amari (2005) list schreibersite (Fe_3P) as a stellar condensate in their table of "expected and observed major element condensates." They suggest conditions of formation as ~1250 K at 10^{-4} atm; however, to our knowledge schreibersite has not yet been observed as a stellar mineral.

Nitrides

Nitrogen, among the most abundant "metal" elements in stars, is a ubiquitous minor element in presolar moissanite, though the only confirmed stellar grains of refractory nitrogen minerals are the silicon nitride, nierite (Si_3N_4).

Nierite (Si_3N_4). Nierite is formed in the ejecta of core-collapse supernovae (Nittler et al. 1995; Hoppe et al. 1996; Lin et al. 2010). The few documented grains of stellar nierite, representing ~2 ppb of the Murchison CM chondrite, display uniform excesses of ^{15}N and ^{28}Si relative to solar values, as well as Ti isotopic anomalies that point to likely origins in Type II supernovae. The Presolar Grain Database, which records 41 analyzed nierite grains (Hynes and Gyngard 2009; see https://presolar.physics.wustl.edu/ accessed 24 Jan 2019), documents distinctive ranges of nitrogen isotopes ($18 < {}^{14}N/{}^{15}N < 190$, compared to 249 for the solar average) and low $^{30}Si/^{28}Si$.

SN-II nierite: Characterized by low $^{14}N/^{15}N$ and $^{30}Si/^{28}Si$ relative to solar averages.

Other possible stellar nitrides. Reports of nanoscale concentrations, inclusions, or subgrains in stellar X-type moissanite include Ti(N,C) and (Mg,Al)N (Groopman and Nittler 2018; Gyngard et al. 2018), as well as an aluminum nitride, possibly AlN (Stroud and Bernatowicz 2005; Hynes et al. 2010). Further chemical and structural characterization will be required before assigning mineral names to these minute features.

Sulfides

Rare stellar sulfide grains of oldhamite (CaS) and iron sulfide, most likely troilite (FeS), have been reported as nanoscale inclusions in graphite and moissanite grains (Hynes 2010; Hynes et al. 2011; Haenecour et al. 2016). These unambiguously stellar inclusions are characterized by anomalous S isotopes, in host grains with anomalous C isotopes.

Oldhamite (CaS). Oldhamite is calculated to be the highest temperature sulfide to condense in the atmosphere of a carbon-rich star (~1300 K at 10^{-4} atm; Lodders and Amari 2005, their Fig. 1). The rarity of oldhamite presolar grains is likely a consequence of two factors: (1) the relatively low abundances of sulfur and calcium in stellar atmospheres of carbon stars, and (2) the solubility of oldhamite in water, which is often used in the preparation of meteorite mineral separates and polished sections.

AGB oldhamite: Hynes (2010) and Hynes et al. (2011) describe 7 anhedral inclusions of oldhamite with diameters from 16 to 40 nm. These subgrains occur as epitaxially aligned inclusions in AGB moissanite (ascribed to "AB"-type, possibly from a J star) grains.

Troilite [?] (FeS). Of special note is a report by Haenecour et al. (2016), who describe a presolar iron sulfide inclusion (80 nm diameter) in a 300-nm-diameter graphite of suspected Type II supernova origins, though an AGB source cannot be ruled out. This observation is surprising, as the highest-temperature iron sulfide, troilite, condenses at a relatively low temperature (~700 K at 10^{-4} atm; Lodders 2003), compared to other confirmed presolar phases. However, the anomalously low $^{33}S/^{32}S$ and $^{34}S/^{32}S$ relative to solar abundances, coupled with the carbon isotope ratio of the graphite (characterized by $^{12}C/^{13}C > 200$), point unambiguously to a stellar origin. Haenecour et al. (2016) suggest that the graphite grain and troilite inclusion originated in a Type II supernova,

with the graphite and troilite condensing in different shells of the ejecta—a scenario consistent with models of supernova heterogeneities (Sarangi and Cherchneff 2015). However, they do not rule out the possibility of an origin in a ~3 solar mass, low-metallicity AGB star.

Given the low condensation temperature of troilite, Lodders (personal communication) suggests "sulfurization" of a stellar iron grain as a plausible alternative explanation. If so, then the troilite grain formed by secondary gas/solid reactions that occurred in reduced AGB winds—a process discussed by Lauretta et al. (1998).

SN-II (?) troilite: Nano-inclusion in graphite, characterized by anomalously negative $\delta^{33}S$ and $\delta^{34}S$ (Haenecour et al. 2016). Note that an AGB origin cannot be ruled out.

Other possible sulfides. Lodders and Amari (2005) list niningerite (MgS) as a stellar condensate in their table of "expected and observed major element condensates." They suggest conditions of formation as ~1050 K at 10^{-4} atm; however, to our knowledge niningerite has not yet been observed as a stellar mineral.

Oxides

Suites of refractory oxide and silicate minerals have long been recognized as constituents of the dusty atmospheres of aging oxygen-rich stars and supernovae, based on astronomical observations of characteristic mid-infrared absorption features (Gillett et al. 1968; Stein et al. 1969; Woolf and Ney 1969; Onaka et al. 1989; Little-Marenin and Little 1990; Sloan and Price 1998; Speck et al. 2000; DePew et al. 2006), with notable advances in resolution and sensitivity following the successful launch of orbiting infrared telescopes (Neugebauer et al. 1984; Waters et al. 1996; Messenger et al. 2003; Nguyen and Zinner 2004; Rieke 2009; Jiang et al. 2013). Nevertheless, the isolation and characterization of oxides and silicates from primitive meteorites has proven challenging. Unlike the acid-insoluble carbon allotropes and carbides, which form a distinctive population of unambiguously stellar minerals, the rare, diminutive grains of stellar oxides and silicates are difficult to distinguish from the ubiquitous background of similar nebular condensates.

Following the fortuitous discovery of a stellar corundum grain with extreme enrichments in ^{17}O coupled with enhanced ^{26}Mg—an unambiguous signature of the decay of short-lived ^{26}Al and a likely consequence of its AGB origins (Hutcheon et al. 1994)—rapid progress was made by the application of automated methods to detect individual oxide and silicate grains with anomalous isotopic values (Huss et al. 1994; Nittler et al. 1994, 1997, 2008; Choi et al. 1998; Nguyen et al. 2007; Takigawa et al. 2014, 2018; Fig. 5). Corundum and amorphous Al_2O_3 dominate the inventory of stellar oxides, with modest numbers of oxide spinel and hibonite grains, as well as minor titanium oxide. The stellar oxide content of meteorites varies widely, with primitive carbonaceous chondrites holding the highest amounts—up to 55 ppm reported by Nguyen et al. (2007).

While efforts to characterize the diversity of stellar oxide and silicate phases are still in progress, several broad groups of these astrominerals have been classified based primarily on oxygen isotope ratios relative to solar averages. Approximately 70% of grains, labeled "Group 1" by Nittler et al. (1997), carry high $^{17}O/^{16}O$ and average or slightly low $^{18}O/^{16}O$—values that point to nucleosynthesis in typical oxygen-rich red giant and AGB stars during and after the first dredge up phase. Variations in stellar mass and initial metallicity play a significant role in the values of $^{17}O/^{16}O$ and $^{18}O/^{16}O$ (e.g., Timmes et al. 1995).

A smaller population of "Group 2" grains, ~15% of all oxides and silicates, display the high $^{17}O/^{16}O$ characteristic of AGB stars, but very low $^{18}O/^{16}O$—a feature initially thought to arise from cool-bottom processing (CBP) from relatively small (<2 solar mass) AGB stars. Note, however, that Lugaro et al. (2017) suggest a similar isotopic signature might arise from a >4 solar mass AGB star, based on a revised experimental determination of the proton-capture rate of ^{17}O (Bruno et al. 2016). By contrast, AGB stars of low mass and low metallicity produce "Group 3" grains (5% of all oxide and silicate samples) that display light oxygen isotopes, with both low $^{17}O/^{16}O$ and low $^{18}O/^{16}O$ relative to solar averages.

The origins of "Group 4" grains (perhaps 10% of all stellar oxides and silicates), with significant excesses of ^{18}O relative to ^{16}O and a range of $^{17}O/^{16}O$, as well as elevated ^{26}Mg coupled with ^{28}Mg depletions, remain a matter of debate. Both AGB stars with high metallicity and low mass and Type II supernovae with a complex mixing history have been invoked (Nittler et al. 1997; Choi et al. 1998; Nguyen and Messenger 2014; Zinner 2014). Finally, rare (less than 1%) "N-type" oxide and silicate grains are thought to arise from classical novae and are characterized by significantly elevated $^{17}O/^{16}O$, while $^{18}O/^{16}O$ is low (Nittler et al. 2008, 2011; Gyngard et al. 2010a, 2011; Nguyen and Messenger 2014).

In conformity with our proposed evolutionary classification system of minerals, we recognize three distinct paragenetic modes for stellar oxide and silicate grains: AGB stars (including Group 1, 2, 3, and perhaps some Group 4 grains), Type II supernovae (including some Group 4 grains), and classic novae (N-type grains).

Corundum (Al_2O_3). The occurrence of stellar corundum was suspected on the basis of a sharp infrared absorption feature at ~13 μm in the spectra of oxygen-rich AGB stars (Onaka et al. 1989; Speck et al. 2000; Takigawa et al. 2015). Corundum condenses at temperatures as high as 1700 K, and is thought to be the first phase to crystallize in the atmospheres of these stars (Grossman 1972; Salpeter 1977). Grains of stellar corundum were first identified in acid residues of meteorites by measurements of oxygen isotope anomalies (Hutcheon et al. 1994; Nittler et al. 1997; Choi et al. 1998; Zinner et al. 2011; Takigawa et al. 2014, 2018). Corundum (α-Al_2O_3) and amorphous aluminum oxide are now known to be common constituents of presolar grains.

A matter of debate has been whether corundum can precipitate directly in its crystalline form in stellar atmospheres, or whether the crystalline form arises later from annealing of amorphous Al_2O_3. This issue was resolved by Takigawa et al. (2018), who describe a single 1.4 μm subhedral grain that represents a primary stellar condensate, formed in the atmosphere of a low- or intermediate-mass AGB star based on its characteristic isotopic signature: elevated ^{17}O (in this case enriched by a factor of ~3) and lower ^{18}O (depleted by a factor of ~25) relative to solar abundances (Fig. 3d). The principal impurity in this grain was magnesium, enriched in ^{26}Mg as a consequence of the rapid decay of short-lived ^{26}Al from *s*-process nucleosynthesis. The relatively large size of this corundum grain, furthermore, suggests that it grew for several years in the extended atmosphere of its parent star. Such "large" grains are particularly subject to radiation pressure and have been invoked in triggering of dust-driven winds from AGB stars (Höfner 2008).

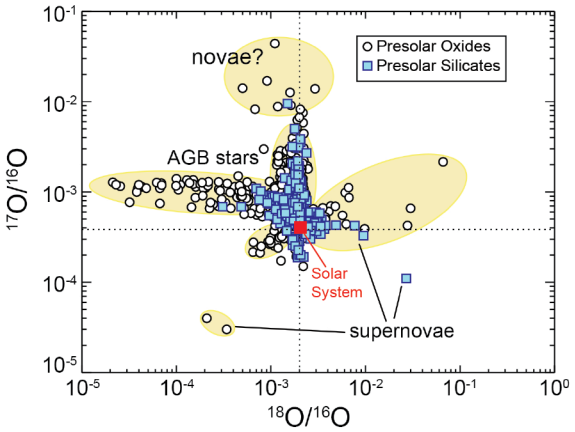

FIGURE 5. Oxygen isotopes in presolar oxides and silicates display extreme isotopic anomalies relative to solar averages. Clustering of these data points to a variety of stellar environments. Courtesy of Nittler et al. (2008) and Zinner (2014). (Color online.)

The more than 250 corundum grains tabulated in the Presolar Grain Database (Hynes and Gyngard 2009; see https://presolar.physics.wustl.edu/ accessed 24 Jan 2019) span the several groups of stellar oxides and silicates proposed by Nittler et al. (1997). Therefore, we recognize three different natural kinds of corundum from stars. It should be noted, however, that relatively few Al_2O_3 grains have been examined by electron diffraction; therefore, the crystallinity of many grains remains uncertain. For example, of two grains studied by Stroud et al. (2004b), one was found to be corundum and the other amorphous Al_2O_3.

AGB corundum: The majority of presolar corundum grains carry the Group 1 isotopic signatures of AGB stars from 1 to <3 solar masses, including elevated $^{17}O/^{16}O$ and normal or slightly low $^{18}O/^{16}O$ (Hutcheon et al. 1994; Nittler et al. 1997; Choi et al. 1998; Takigawa et al. 2014). In addition, approximately one in six stellar corundum grains display elevated $^{17}O/^{16}O$ and very low $^{18}O/^{16}O$ characteristic of Group 2 late-stage cool-bottom processing in AGB stars (Davis 2011; Takigawa et al. 2014). Some grains also incorporate significant ^{26}Mg, a consequence of short-lived ^{26}Al. Takigawa et al. (2018) describe a euhedral Group 2 AGB corundum grain, 1.4 μm in diameter, that suggests extended growth of a pristine crystal in the stellar atmosphere. Finally, a small population of Group 3 stellar corundum grains has both low $^{17}O/^{16}O$ and low $^{18}O/^{16}O$—features ascribed to AGB stars of relatively low mass and low metallicity (Nittler et al. 2008).

SN-II corundum: Approximately one in 10 stellar corundum grains have low $^{17}O/^{16}O$ and low $^{18}O/^{16}O$, similar to Group 3 AGB corundum, but they also incorporate significant ^{26}Mg, ^{44}Ca, and ^{49}Ti, which point to origins in a Type II supernova (Choi et al. 1998; Nittler et al. 2008).

CNova corundum: Fewer than 1% of stellar corundum grains have oxygen isotope signatures associated with origins in classical novae: very high $^{17}O/^{16}O$ combined with low $^{18}O/^{16}O$ (Nittler et al. 2008).

Amorphous Al_2O_3. Amorphous Al_2O_3, which was verified on the basis of electron diffraction by Stroud et al. (2004b), arises from rapid cooling of Al-O rich zones in an AGB stellar atmosphere. Takigawa et al. (2018) suggest that the amorphous form could subsequently anneal to corundum.

AGB amorphous Al_2O_3: Origins of amorphous Al_2O_3 in an O-rich AGB star was inferred from anomalously elevated $^{17}O/^{16}O$, as well as $^{26}Mg/^{24}Mg$.

Eskolaite (Cr_2O_3). Croat et al. (2008) describe two SN-II graphite grains with 50-nm-diameter inclusions of chromium oxide and trigonal unit-cell parameters matching those of eskolaite. Additional nano-inclusions rich in Cr-oxide display cubic unit-cell parameters, perhaps corresponding to CrO.

SN-II eskolaite: Occurs as nanoscale inclusions in SN-II graphite (Croat et al. 2008).

Titanium oxide (TiO_2). Nittler et al. (2008) identified four grains of TiO_2 with elevated ^{17}O, thus pointing to origins in an AGB star, with subsequent work by Bose et al. (2010a) and Zega et al. (2011). Thus far, no electron diffraction data are available on the polymorph of AGB TiO_2 (L. Nittler, personal communications). Croat et al. (2011) performed electron diffraction experiments on 52 TiO_2 inclusions in SN-II graphite and employed electron diffraction to confirm that specimens possessed the tetragonal rutile structure. Groopman and Nittler (2018) subsequently employed Ti-XANES to identify a presolar rutile inclusion in a graphite grain of presumed supernova origins, based on its high $^{12}C/^{13}C$ and high $^{18}O/^{16}O$ relative to solar abundances.

AGB TiO_2: Characterized by high $^{17}O/^{16}O$ (Nittler et al. 2008; Bose et al. 2010a; Zega et al. 2011); the polymorph is not yet resolved.

SN-II rutile: Inclusions in SN-II graphite with elevated $^{12}C/^{13}C$ and $^{18}O/^{16}O$ (Groopman and Nittler 2018). TEM analyses reveal tetragonal grains with rutile unit-cell parameters (Croat et al. 2011).

Magnetite (Fe_3O_4). Croat et al. (2008) reported magnetite inclusions in stellar graphite. A single crystal of stellar magnetite (maximum dimension ~750 nm) was subsequently described by Zega et al. (2015), who measured elevated $^{17}O/^{16}O$ relative to solar abundances. They postulate that the grain formed by oxidation of an iron grain in the O-rich atmosphere of a solar metallicity AGB star (~2 stellar mass) during the first dredge up phase over time scales of 10^4 to 10^6 years. If so, then AGB magnetite would represent one of only three plausible secondary stellar minerals (in contrast to a primary condensate), the others being troilite (FeS; Haenecour et al. 2016) and shock-produced $MgSiO_3$ silicate perovskite (Vollmer et al. 2007).

AGB magnetite: Magnetite with elevated $^{17}O/^{16}O$ relative to solar abundances; likely formed by secondary gas/solid oxidation reactions of stellar iron.

Spinel ($MgAl_2O_4$). Stellar oxide spinel grains were initially recognized as presolar grains because of their anomalous oxygen isotope values—notably enrichment in ^{17}O and depletion in ^{18}O relative to solar averages (Nittler et al. 1994; Choi et al. 1998). Gyngard et al. (2010a) subsequently analyzed 38 spinel grains from the Murray CM2 meteorite. The majority have isotope anomalies consistent with AGB origins, but one grain with extreme enrichments in ^{17}O, ^{25}Mg, and ^{26}Mg is thought to have formed in a supernova environment.

Zega et al. (2014a) described automated analyses of the acid-resistant fraction of several chondrite meteorites, in which they identified 37 oxide spinel grains. The majority of these grains were close to Mg-Al-spinel, but five grains displayed compositions in

the Fe-Cr-chromite field (see below). From this suite of samples, they selected four grains, each up to 0.5 μm in maximum diameter, for detailed study. All of the 37 spinel grains identified display isotopic anomalies consistent with a presolar origin, notably ^{17}O enrichment consistent with origins in an AGB star somewhat more massive than the Sun and with approximately solar metallicity. Zega et al. (2014a) estimated the host star's mass to be 1.2 to 1.4 times than the Sun; note, however, that revised experimental measurements of nuclear reaction rates, for example the ^{17}O's proton-capture rate (Bruno et al. 2016), may affect estimates of AGB stellar masses (Lugaro et al. 2017). Three of these grains are Mg-Al spinel with minor Fe and Cr; one with minor Ca as well; for example, $(Mg_{0.98},Fe_{0.01})(Al_{1.94}Cr_{0.06})O_4$. Pure Mg-Al spinel condenses at 1161 K at 10^{-6} atm and 1221 K at 10^{-3} atm, respectively. Note that stacking disorder observed in TEM studies could point to grain-to-grain impact-induced strain in the stellar atmosphere. Thus, while high pressures do not appear to play any significant role in presolar grain formation, transient events may influence their microstructures.

AGB spinel: The majority of stellar spinel samples are typical of Group 1 grains, displaying the high $^{17}O/^{16}O$ characteristic of AGB stars (Choi et al. 1998; Gyngard et al. 2010a; Zega et al. 2014a).

SN-II spinel: Nittler et al. (2008) and Gyngard et al. (2010a) describe Group 4 oxide spinel grains with high $^{18}O/^{16}O$, low ^{25}Mg, and high ^{26}Mg—characteristics that are ascribed to a Type II supernova origin.

CNova spinel: A single grain reported by Gyngard et al. (2010a) has extreme enrichments in ^{17}O, ^{25}Mg, and ^{26}Mg, likely condensed from classic nova ejecta.

Chromite ($Fe^{2+}Cr_2O_4$). Five grains studied by Nittler et al. (2005) and Zega et al. (2014a) are Fe-Cr-rich chromite. One of the grains is a composite with an average composition $[(Fe_{0.67}Mg_{0.31}Ni_{0.02})(Cr_{1.58}Al_{0.21}Mg_{0.06}Ti_{0.13})O_4]$, close to chromite composition.

AGB chromite: Zega et al. (2014a) describe 5 chromite grains with high $^{17}O/^{16}O$ and low $^{18}O/^{16}O$ relative to solar averages.

Hibonite ($CaAl_{12}O_{16}$). Prior to 1999, the refractory calcium aluminate hibonite [ideally $CaAl_{12}O_{19}$, but given misleadingly by IMA as $(Ca,Ce)(Al,Ti,Mg)_{12}O_{19}$] was assumed by most researchers to be exclusively a primary condensate in the solar nebula. Hibonite is a significant component of calcium aluminum inclusions (CAIs) from chondrite meteorites and specimens from several carbonaceous chondrite meteorites have been studied intensively (Zinner et al. 1986; Fahey et al. 1987; Hinton et al. 1988; Ireland 1988, 1990; Choi et al. 1999; Nittler et al. 2008; Zega et al. 2011; Han et al. 2015). Experimental evidence suggests that corundum and hibonite are among the earliest oxide condensates in a solar nebula, with reported condensation temperatures ranging from 1730 to 1780 K (Wood and Hashimoto 1993; Yoneda and Grossman 1995; Ebel and Grossman 2000; see Ebel 2006 for an overview)—relationships that will be examined in Part II of this series. However, the report by Choi et al. (1999) of two meteoritic hibonite grains with high $^{17}O/^{16}O$ and high ^{26}Mg confirmed the AGB origins of a small fraction of the smallest hibonite grains in chondrites. Subsequent analyses by Nittler et al. (2008) and Zega et al. (2011), including hibonite grains with compositions in the $Ca(Mg,Ti,Al)_{12}O_{19}$ field, point to origins in both AGB stars and Type II supernovae. In addition, Nittler et al. (2011) described a Group 3 hibonite grain with significant depletions in both ^{17}O and ^{18}O relative to solar averages, as well as low $^{25}Mg/^{24}Mg$—an unusual combination not easily ascribed to any single stellar origin.

AGB hibonite: The majority of stellar hibonite specimens are typical Group 1 grains, characterized by high $^{17}O/^{16}O$, average to low $^{18}O/^{16}O$, and high ^{26}Mg and ^{41}K—the latter from ^{41}Ca decay (Choi et al. 1999; Nittler et al. 2008; Zega et al. 2011). In addition, one unusual Group 3 hibonite grain displays significant depletions in both ^{17}O and ^{18}O relative to solar averages, as well as low $^{25}Mg/^{24}Mg$ (Nittler et al. 2011).

SN-II hibonite: A few Group 4 stellar hibonite grains display high $^{18}O/^{16}O$, as well as elevated ^{26}Mg and ^{41}K (Nittler et al. 2008; Zega et al. 2011), characteristic of core-collapse supernovae.

Other possible oxide phases. Additional potential stellar oxide phases include unidentified iron oxides (Floss et al. 2008; Bose et al. 2010b); a cubic chromium oxide, possibly CrO (Croat et al. 2008); as well as possible Ca-Al oxide and Mg-Cr oxide grains (Nittler et al. 2008), though no definitive identifications of these phases are yet forthcoming. In addition, Stroud et al. (2004b) report evidence for a non-corundum hexagonal polymorph of Al_2O_3.

Silicates

Amorphous silicate phases have been recognized as an important, if not dominant, component of the atmospheric dust produced by oxygen-rich evolved AGB stars, based on detection of distinctive infrared features (Woolf and Ney 1969; Treffers and Cohen 1974; T.W. Jones and Merrill 1976; Speck et al. 2000; McAdam et al. 2018). Higher resolution studies by Waters et al. (1996) using the Infrared Space Observatory confirmed the presence of crystalline silicates, as well—work that has been amplified by measurements with subsequent orbiting infrared observatories (e.g., Jiang et al. 2013).

The first unambiguously stellar silicate grains were discovered in interplanetary dust particles (Messenger et al. 2003), with subsequent identification in both polished sections of meteorites (Mostefouai and Hoppe 2004; Nagashima et al. 2004; Nguyen and Zinner 2004) and Antarctic micrometeorites (Yada et al. 2008). Numerous subsequent publications (Zinner 2014 and references therein) record more than 250 meteoritic silicate grains with extreme isotopic anomalies that formed in the atmospheres of stars. These investigations suggest that stellar silicate grains, though typically less than 1 μm in diameter and with many grains smaller than 100 nm diameter, represent the most abundant group of stellar minerals—up to a few hundred parts per million in primitive chondrite meteorites, compared to ~30 ppm for stellar moissanite (Zinner 2014, his Fig. 17; Nittler et al. 2018b). Most stellar silicate grains appear to have AGB origins, though at least one supernova olivine grain with excess ^{18}O and depleted ^{17}O has been identified (Messenger et al. 2005).

A significant challenge in the systematic classification of stellar silicates is their diminutive scale, which makes chemical and structural analysis difficult. Major element analysis of Mg, Fe, and Si reveal several grains with pyroxene or olivine stoichiometry, with significant iron content in all measurements (possibly a consequence of subsequent alteration). However, more than half of analyzed grains appear to be nonstoichiometric and may represent amorphous silicates (Floss and Stadermann 2009, 2012; Vollmer et al. 2009; Bose et al. 2010a; Nguyen et al. 2010; Kemper et

al. 2011; see Zinner 2014, his Fig. 18). The complexity of some stellar oxide and silicate grains is represented by a zoned AGB (Group 1) grain with an Al-Ca-Ti oxide core and Mg-Ca-silicate mantle (Leitner et al. 2018), as well as other composite oxide-silicate grains (Vollmer et al. 2013; Nguyen et al. 2016; Nittler et al. 2018b). As the identification and characterization of stellar silicates is still in its infancy, we recognize olivine and enstatite as the only two confirmed IMA-approved species.

Forsterite (Mg_2SiO_4). Based on astronomical observations, Mg-rich olivine is the most common stellar crystalline silicate, estimated to exceed the quantity of pyroxene by a factor between 2 and 3 (Kemper et al. 2004; O.C. Jones et al. 2012). Most confirmed presolar olivine grains display characteristics of AGB stars, though distinctive SN-II grains have also been observed (Zinner 2014). Note that a significant fraction of stellar forsterite may be subsequently lost through amorphization by shock and/or irradiation (Brucato et al. 2004).

AGB forsterite: Mostefouai and Hoppe (2004) described three forsterite grains with elevated ^{17}O, typical of AGB stars. Additional reports of stellar AGB olivine include Busemann et al. (2009), Vollmer et al. (2009), Zega et al. (2014b; notably Ca-bearing), Nguyen and Messenger (2016), and Nittler et al. (2018b).

SN-II forsterite: Messenger et al. (2005) describe a single grain of olivine with high $^{18}O/^{16}O$ and low $^{17}O/^{16}O$, characteristic of supernova origins.

Enstatite ($MgSiO_3$). Magnesium silicate pyroxene is the second important crystalline stellar silicate phase, based on both astronomical observations and analyses of isotopically anomalous presolar silicate grains (Mostefouai and Hoppe 2004; Zinner 2014). Note that while enstatite may condense directly, Carrez et al. (2002b) suggested that enstatite could also crystallize from amorphous silicate under the influence of electron radiation in a circumstellar environment.

AGB enstatite: Mostefouai and Hoppe (2004) described four pyroxene grains with the characteristic elevated $^{17}O/^{16}O$ of AGB origins. Subsequent studies have documented dozens of additional examples, a few of which have been confirmed by TEM analyses to have the pyroxene structure, though most identifications of "enstatite" are based on bulk compositions with (Mg + Fe) ~ Si (Floss and Stadermann 2009, 2012; Bose et al. 2010a; Vollmer et al. 2013; Nguyen et al. 2016; see also Zinner 2014, his Fig. 18).

SN-II enstatite: One pyroxene grain examined by Mostefouai and Hoppe (2004) displayed normal $^{17}O/^{16}O$ and extremely elevated $^{18}O/^{16}O$, thought to result from Type II supernovae.

Bridgmanite ($MgSiO_3$). Of special interest is a grain of bridgmanite, the high-pressure, perovskite-structured polymorph of $MgSiO_3$, which possibly formed as the result of a high-velocity impact of a stellar shock wave on enstatite (Vollmer et al. 2007). If so, then stellar bridgmanite represents a secondary alteration phase. The grain possesses high $^{17}O/^{16}O$ and low $^{18}O/^{16}O$, perhaps reflecting an origin in a low-mass, solar metallicity AGB star during and after the first dredge up phase.

AGB bridgmanite: High-pressure $MgSiO_3$ polymorph, perhaps the consequence of shock alteration of AGB enstatite.

Amorphous silicate. More than half of studied presolar silicate grains are amorphous (Kemper et al. 2004; Messenger et al. 2003; Zinner 2014), and most of those are non-stoichiometric phases with compositions intermediate to those of forsterite and enstatite (e.g., Zinner 2014, his Fig. 18). The great majority of these grains display the elevated $^{17}O/^{16}O$ associated with AGB stars. Note, however, that Kemper et al. (2004) suggest that Type II supernovae may be a significant additional source of amorphous silicates. Amorphous silicates may condense directly in the stellar atmosphere, or they may occur as a result of subsequent irradiation and/or shocks in the circumstellar/interstellar medium (A.P. Jones et al. 1994; Demyk et al. 2000; Carrez et al. 2002a; Brucato et al. 2004; A.P. Jones 2007).

AGB amorphous Mg-Fe silicate: Amorphous Mg-Fe silicate compositions with elevated $^{17}O/^{16}O$.

Network graph of stellar minerals

Network graphs provide a useful method to visualize relationships among varied minerals and their attributes (Morrison et al. 2017). Figure 6 displays a bipartite force-directed network graph of stellar minerals, in which 27 phases—22 IMA approved mineral species, two additional crystalline phases not yet recognized by IMA (MoC and Fe_7C_3), plus three amorphous condensed phases (C, Al_2O_3, and silicate)—are represented by diamond-shaped nodes. These mineral nodes are linked to three types of stars (AGB, SN-II, and CNova) represented by star-shaped nodes. Compositional information is conveyed by mineral node colors: black (C-bearing), green (not C or O), blue (contains O, but not Si), and red (contains Si+O).

This visual representation of all confirmed stellar minerals underscores several important trends. First, all of these stellar phases (and the great majority of confirmed stellar mineral grains) are formed in the atmospheres of AGB stars (17 phases) and/or Type II supernovae (19 phases). Furthermore, 23 types of condensed stellar phases are only known from these sources. By contrast, only four minerals are confidently ascribed to classical novae: graphite, moissanite, corundum, and spinel. Both AGB stars and Type II supernovae produce a wide compositional

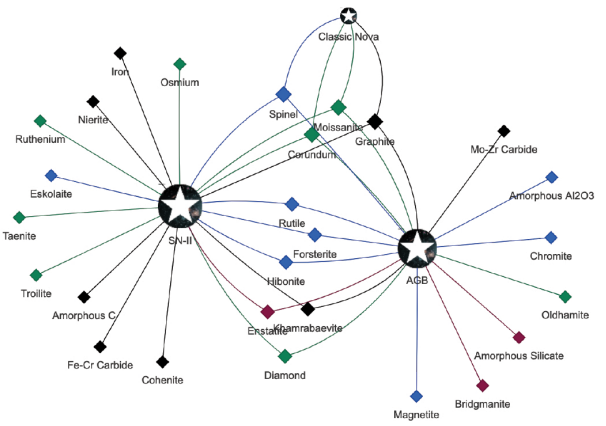

FIGURE 6. Bipartite force-directed network graph (Morrison et al. 2017) of stellar minerals linked to their host stars. Diamond-shaped nodes represent condensed crystalline and amorphous phases [black (C-bearing), green (not C or O), blue (contains O, but not Si), and red (contains Si + O)], whereas star-shaped nodes represent three types of host stars—asymptotic giant branch stars (AGB), Type II supernovae (SN-II), and classical novae (CNova). The sizes of the host star nodes correspond to the number of links to other nodes. Courtesy of Anirudh Prabhu, RPI. (Color online.)

and silicates.

Graphite, moissanite, corundum, and spinel are the only phases thus far identified from all three of these stellar hosts. This uneven distribution of stellar minerals among types of stars in part reflects the prodigious production of stardust in AGB planetary nebulas and Type II supernovae.

Trace and minor elements in stellar minerals

The 27 phases represented by the known inventory of stellar minerals incorporate only 11 different abundant chemical elements and 6 minor elements as essential constituents (Fig. 1). An important unanswered question relates to the scores of other chemical elements that are not represented as significant constituents during the pre-solar phase of mineral evolution. All of these elements must be present in stardust particles, but where do they reside? One possible answer lies in the proposal of Lodders and Amari (2005; their Table 9), who suggested that several refractory minerals may await discovery as stellar minerals. Among their proposed condensates are gehlenite ($Ca_2Al_2SiO_7$), grossite ($CaAl_4O_7$), anorthite ($CaAl_2Si_2O_8$), perovskite ($CaTiO_3$), iron silicide (FeSi), and aluminum nitride (AlN), as well as phases of S [niningerite (MgS), daubréelite ($FeCr_2S_4$), alabandite (Mn,Fe)S], P [schreibersite $(Fe,Ni)_3P$], Na [albite ($NaAlSi_3O_4$)], K [orthoclase ($KAlSi_3O_4$)], and Cl {sodalite [$Na_4(AlSiO_4)_3Cl$]}.

However, for a variety of less abundant elements at least three additional structural roles have likely occurred. A few elements are close proxies for common constituents of the ur-minerals, and thus were easily incorporated into the adaptable lattices of these earliest minerals (Table 1). For example, gallium substitutes for aluminum, cobalt for iron, and manganese for calcium and/or iron. This propensity for some rarer elements to follow their chemically similar but more abundant neighbors may result in a relative paucity of mineral species for many of these elements (e.g., Christy 2015; Hazen et al. 2015).

A second possibility is that rarer elements are "swept up" during crystallization and thus are incorporated as defect sites in crystals. Nitrogen and boron, for example, are common defect elements in diamond, while N and Ti are ubiquitous in stellar moissanite. The range of possible single-atom defects in crystals is at present poorly constrained but deserves further study.

The third likely locus for trace and minor elements in pre-solar minerals is grain boundary regions in complex polycrystalline and/or amorphous composite stellar grains. Structural and compositional details of grain boundaries are lacking. In particular, it is not known the extent to which these regions are amorphous vs. nano-crystalline. It is plausible that some moderately rare "minerals" form as local concentrations with dozens to hundreds of unit cells—"phases" that may be revealed as atomic-scale-resolution microscopy becomes more widely applied to mineral systems (e.g., Ma et al. 2013, 2017; Rubin and Ma 2017).

Implications

The fascinating discipline of stellar mineralogy holds two important lessons for the field of mineralogy. First, a rigorous, quantitative methodology is needed to identify discrete natural kinds of minerals. In the case of astrominerals, we need to adopt and modify data-driven methodologies that rely on the richness of idiosyncratic, diagnostic attributes of presolar grains: trace and minor elements, ratios of isotopes, structural defects, inclusions, external morphologies, and other attributes that derive from their specific paragenetic histories and that distinguish them from other populations. We suggest that multi-dimensional analysis based on natural kind clustering of large, reliable, open-access data resources will reveal quantitative discriminants that place our systematic classification of stellar minerals on a secure footing. For example, we are now expanding the Presolar Grain Database (Hynes and Gyngard 2009; see https://presolar.physics.wustl.edu/) to investigate more than 20 000 stellar moissanite grain analyses based on $^{12}C/^{13}C$, $^{14}N/^{15}N$, $^{30}Si/^{28}Si$, $^{29}Si/^{28}Si$, and such trace isotopes as ^{26}Mg, ^{44}Ca, and ^{49}Ti. Preliminary cluster analysis reveals several discrete populations; however, an important caveat relates to the degree of separation or "distance" both within and between different presumed clusters of stellar mineral grains. We hope to determine whether clusters based on attributes of stardust grains are non-overlapping in multi-dimensional composition space, as opposed to possessing variations that arise from continuous ranges of attributes in complex temperature-pressure-composition space. In either eventuality, cluster analysis will enhance our understanding of the dynamic, evolving sources of stardust.

Second, these varied, ancient condensed stellar phases underscore the need for an evolutionary system of mineralogy, which complements the existing IMA protocols based on idealized end-member compositions and crystal structures. Stellar minerals represent at least 22 IMA-approved mineral species, but their remarkable isotopic and morphological idiosyncrasies point to more than 40 "natural kinds" that are quite distinct from their more familiar terrestrial counterparts. Minerals that condensed from the atmospheres of stars are fundamentally distinct in chemistry, isotopic composition, morphology, and associations from more recent terrestrial examples of the same IMA-approved species. Stellar mineralogy also embraces the most ancient of a growing inventory of condensed non-crystalline phases that are important in all eras of the mineral evolution of Earth and other planets but have received scant attention in the systematic consideration of evolving planetary systems.

For more than 13 billion years, the stardust of the earliest stage of mineral evolution has enriched the interstellar medium, comprising a significant fraction of the molecular clouds and nebulas where new generations of stars, and their diverse retinue of mineral-rich planets and moons, are born. In the process, new minerals, including ices and other low-temperature condensates, expanded the cosmic mineralogical inventory. These far-flung interstellar processes were the prelude to the condensation and/or low-pressure melting in the solar nebula of a growing inventory of minerals—phases that are preserved as chondrules, refractory inclusions, and the matrix of chondrite meteorites. That phase of mineral evolution will be the subject of the second and the third contributions in this series.

In this and subsequent contributions, the guiding principle of the evolutionary system of mineralogy is that each mineral sample is a rich storehouse of information. Each specimen possesses myriad physical and chemical attributes that point to its origin and subsequent alteration pathways through space and time. We thus embrace the inherent "messiness" of nature—the complexities that reveal the evolution of stars, planets, minerals, and life.

ACKNOWLEDGMENTS

Throughout the preparation of this paper, we have benefitted from the generous advice and deep expertise of Larry R. Nittler, a pioneer in astromineralogy, who was an early reviewer of this contribution and a constant adviser during its revisions. We are grateful to Anirudh Prabhu for providing the network diagram of the Evolutionary System of stellar mineralogy. Denton Ebel and an anonymous reviewer offered thoughtful comments and suggestions that have greatly improved this study. In addition, we thank Conel M.O'D. Alexander, Asmaa Boujibar, Carol Cleland, Robert T. Downs, Olivier Gagné, Pierre Haenecour, Peter Heaney, Samantha Howell, Sergey Krivovichev, Chao Liu, Katharina Lodders, Michael Walter, and Shuang Zhang for thoughtful discussions and comments.

FUNDING

This publication is a contribution to the Deep Carbon Observatory. Studies of mineral evolution and mineral ecology are supported by the Deep Carbon Observatory, the Alfred P. Sloan Foundation, the W.M. Keck Foundation, the John Templeton Foundation, the NASA Astrobiology Institute, a private foundation, and the Carnegie Institution for Science. Any opinions, findings, or recommendations expressed herein are those of the authors and do not necessarily reflect the views of the National Aeronautics and Space Administration.

REFERENCES CITED

Abel, T., Bryan, G.L., and Norman, M.L. (2002) The formation of the first stars in the universe. Science, 295, 93–98.

Abia, C., and Isern, J. (2000) The chemical composition of carbon stars. II. The J-type stars. The Astrophysical Journal, 536, 438–449.

Alexander, C.M.O'D. (1993) Presolar SiC in chondrites: How variable and how many sources? Geochimica et Cosmochimica Acta, 57, 2869–2888.

Alexander, C.M.O'D., and Nittler, L.R. (1999) The galactic evolution of Si, Ti, and O isotopic ratios. The Astrophysical Journal, 519, 222–235.

Alexander, C.M.O'D., Swan, P., and Walker, R.M. (1990) In situ measurement of interstellar silicon carbide in two CM chondrite meteorites. Nature, 348, 715–717.

Amari, S. (2014) Recent progress in presolar grain research. Mass Spectrometry, 3, 6 pp. doi: 10.5702/massspectrometry.S0042.

Amari, S., Anders, E., Virag, A., and Zinner, E. (1990) Interstellar graphite in meteorites. Nature, 345, 238–240.

Amari, S., Hoppe, P., Zinner, E., and Lewis, R.S. (1992) Interstellar SiC with unusual isotopic compositions: Grains from a supernova? The Astrophysical Journal, 394, L43–L46.

Amari, S., Lewis, R.S., and Anders, E. (1994) Interstellar grains in meteorites: I. Isolation of SiC, graphite, and diamond; size distributions of SiC and graphite. Geochimica et Cosmochimica Acta, 58, 459–470.

Amari, S., Zinner, E., and Lewis, R.S. (1995a) Large ^{18}O excesses in circumstellar graphite grains from Murchison meteorite: Indication of a massive-star origin. The Astrophysical Journal Letters, 447, L147–L150.

Amari, S., Lewis, R.S., and Anders, E. (1995b) Interstellar grains in meteorites: III. Graphite and its noble gases. Geochimica et Cosmochimica Acta, 59, 1411–1426.

Amari, S., Hoppe, P., Zinner, E., and Lewis, R.S. (1995c) Trace-element concentrations in single circumstellar silicon carbide grains from the Murchison meteorite. Meteoritics, 30, 679–693.

Amari, S., Zinner, E., and Lewis, R.S. (1999) A singular presolar SiC grain with extreme ^{29}Si and ^{30}Si excesses. The Astrophysical Journal, 517, L59–L62.

Amari, S., Nittler, L.R., Zinner, E., Gallino, R., Lugaro, M., and Lewis, R.S. (2001a) Presolar SiC grains of type Y: Origin from low metallicity asymptotic giant branch stars. The Astrophysical Journal, 546, 248–266.

Amari, S., Nittler, L.R., Zinner, E., Lodders, K., and Lewis, R.S. (2001b) Presolar SiC grains of Type A and B: Their isotopic compositions and stellar origins. The Astrophysical Journal, 559, 463–483.

Amari, S., Gao, X., Nittler, L.R., Zinner, E., José, J., Hernandez, H., and Lewis, R.S. (2001c) Presolar grains from novae. The Astrophysical Journal, 551, 1065–1072.

Amari, S., Zinner, E., and Lewis, R.S. (2004) Comparison study of presolar graphite separates KE3 and KFA1 from the Murchison meteorite. Lunar and Planetary Science, 35, #2103.

Amari, S., Gallino, R., and Pignatari, M. (2006) Presolar graphite from the Murchison meteorite: Noble gases revisited. Lunar and Planetary Science, 37, #2409.

Bailey, K.D. (1994) Typologies and Taxonomies: An Introduction to Classification Techniques. Studies in Quantitative Applications in the Social Sciences, 102. SAGE Publications.

Bernatowicz, T.J., Fraundorf, G., Ming, T., Anders, E., Wopenka, B., Zinner, E., and Fraundorf, P. (1987) Evidence for interstellar SiC in the Murray carbonaceous chondrite. Nature, 330, 728–730.

Bernatowicz, T.J., Amari, S., and Lewis, R.S. (1992) TEM studies of a circumstellar rock. Lunar and Planetary Science, 23, 91–92.

Bernatowicz, T.J., Cowsik, R., Gibbons, P., Loddeers, K., Fegley, B., Amari, S., and Lewis, R. (1996) Constraints on stellar grain formation from presolar graphite in the Murchison meteorite. The Astrophysical Journal, 472, 760–782.

Bernatowicz, T.J., Bradley, J., Amari, S., Messenger, S., and Lewis, R. (1999) New kinds of massive star condensates in a presolar graphite from Murchison. Lunar and Planetary Science Conference, 30, #1392.

Bernatowicz, T.J., Messenger, S., Pravdivtseva, O., Swan, P., and Walker, R.M. (2003) Pristine presolar silicon carbide. Geochimica et Cosmochimica Acta, 67, 4679–4691.

Bernatowicz, T.J., Croat, T.K., and Daulton, T.L. (2006) Origin and evolution of carbonaceous grains in stellar environments. In D.S. Lauretta and H.Y. McSween Jr., Eds., Meteorites and the Early Solar System II, pp. 109–126. University of Arizona Press.

Bertulani, C.A. (2013) Nuclei in the Cosmos. World Scientific.

Bildsten, L. (1998) Thermonuclear burning on rapidly accreting neutron stars. In R. Buccheri, J. van Paradijs, and M.A. Alpar, Eds., The Many Faces of Neutron Stars. Kluwer, pp. 419B.

Bose, M., Floss, C., and Stadermann, F.J. (2010a) An investigation into the origin of Fe-rich presolar silicates in Acfer 094. The Astrophysical Journal, 714, 1624–1636.

Bose, M., Zhao, X., Floss, C., Stadermann, F.J., and Lin, Y. (2010b) Stardust material in the paired enstatite chondrites: SAH 97096 and SAH 97159. Proceedings of Science, (NIC-XI) 138.

Boulanger, F., Joblin, C., Jones, A., Madden, S., and Tielens, A.G.G.M. (2009) Infrared spectroscopy of interstellar dust. European Astronomical Society Publications Series, 35, 33–56.

Bowman, J.D., Rogers, A.E.E., Monsalve, R.A., Mozdzen, T.J., and Mahesh, N. (2018) An absorption profile centred at 78 megahertz in the sky-averaged spectrum. Nature, 555, 67–70.

Boyd, R. (1991) Realism, anti-foundationalism and the enthusiasm for natural kinds. Philosophical Studies, 61, 127–148.

——— (1999) Homeostasis, species, and higher taxa. In R. Wilson, Ed., Species: New Interdisciplinary Essays, pp. 141–186. Cambridge University Press.

Brucato, J.R., Strazzulla, G., Baratta, G., and Colangeli, L. (2004) Forsterite amorphisation by ion irradiation: Monitoring by infrared spectroscopy. Astronomy & Astrophysics, 413, 395–401.

Bruno, C.G., Scott, D.A., Aliotta, M., Fortmicola, A., Best, A., and 30 others (2016) Improved direct measurement of the 65 keV resonance strength in the $^{17}O(p,alpha)^{14}N$ reaction at LUNA. Physical Review Letters, 117, 142502.

Burbidge, E.M., Burbidge, G.R., Fowler, W.A., and Hoyle, F. (1957) Synthesis of the elements in stars. Review of Modern Physics, 29, 547–650.

Burke, E.A.J. (2006) The end of CNMMN and CCM—Long live the CNMNC! Elements, 2, 388.

Busemann, H., Nguyen, A.N., Cody, G.D., Hoppe, P., Kilcoyne, A.L.D., Stroud, R.M., Zega, T., and Nittler, L.R. (2009) Ultra-primitive interplanetary dust particles from the comet 26P/Grigg-Skjellerup dust strean collection. Earth and Planetary Science Letters, 288, 44–57.

Caffee, M.W., Hohenberg, C.M., Swindle, T.D., and Goswami, J.N. (1987) Evidence in meteorites for an active early sun. The Astrophysical Journal Letters, 313, L31–L35.

Cameron, A.G.W. (1957) Nuclear reactions in stars and nucleogenesis. Publications of the Astronomical Society of the Pacific, 69, 201–222.

Carrez, P., Demyk, K., Cordier, P., Gengembre, L., Grimblot, J., D'Hendecourt, L., Jones, A.P., and Leroux, H. (2002a) Low-energy helium ion irradiation-induced amorphization and chemical changes in olivine: Insights for silicate dust evolution in the interstellar medium. Meteoritics & Planetary Science, 37, 1599–1614.

Carrez, P., Demyk, K., Leroux, H., Cordier, P., Jones, A.P., and D'Hendecourt, L. (2002b) Low-temperature crystallisation of $MgSiO_3$ glasses under electron irradiation: Possible implications for silicate dust evolution in circumstellar environments. Meteoritics & Planetary Science, 37, 1615–1622.

Carroll, B.W., and Ostlie, D.A. (2017) An Introduction to Modern Astrophysics, ed. 2. Cambridge University Press.

Chandrasekhar, S. (1931) The maximum mass of ideal white dwarfs. The Astrophysical Journal, 74, 81–82.

Cheung, R. (2006) Silicon Carbide Microelectromechanical Systems for Harsh Environments. Imperial College Press.

Chigai, T., Yamamoto, T., and Kozasa, T. (2002) Heterogeneous condensation of presolar titanium carbide core-graphite mantle spherules. Meteoritics & Planetary Science, 37, 1937–1951.

Choi, B.-G., Huss, G.R., Wasserburg, G.J., and Gallino, R. (1998) Presolar corundum and spinel in ordinary chondrites: Origins from AGB stars and a supernova. Science, 282, 1284–1289.

Choi, B.-G., Wasserburg, G.J., and Huss, G.R. (1999) Circumstellar hibonite and corundum and nucleosynthesis in asymptotic giant branch stars. The Astrophysical Journal, 522, L133–L136.

Christy, A.G. (2015) Causes of anomalous mineralogical diversity in the Periodic Table. Mineralogical Magazine, 79, 33–49.

Clayton, D.D. (1975) Extinct radioactivities: Trapped residuals of presolar grains. The Astrophysical Journal, 199, 765.

——— (1978) Precondensed matter: Key to the early solar system. Moon and Planets, 19, 109–137.

——— (1983) Principles of Stellar Evolution and Nucleosynthesis. University of Chicago Press.

——— (1997) Placing the sun and mainstream SiC particles in galactic chemodynamic evolution. The Astrophysical Journal, 484, L67–L70.

——— (2003) Presolar galactic merger spawned the SiC mainstream. The Astrophysical Journal, 598, 313–324.

Clayton, D.D., and Nittler, L.R. (2004) Astrophysics with presolar stardust. Annual Review of Astronomy & Astrophysics, 42, 39–78.

Clayton, D.D., and Ward, R.A. (1978) S-process studies: Xenon and krypton isotopic abundances. The Astrophysical Journal, 224, 1000–1006.
Clayton, D.D., Meyer, B.S., Sanderson, C.I., Russell, S.S., and Pillinger, C.T. (1995) Carbon and nitrogen isotopes in type II supernova diamonds. The Astrophysical Journal, 447, 894–905.
Coulter, D.A., Foley, R.J., Kilpatrick, C.D., Drout, M.R., Piro, A.L., Shappee, B.J., Siebert, M.R., Simon, J.D., Ulloa, N., Kasen, D., and others. (2017) Swope Supernova Survey 2017a (SSS17a), the optical counterpart to a gravitational wave source. Science, 358, 1556–1558.
Croat, T.K., Bernatowicz, T., Amari, S., Messenger, S., and Stadermann, F.J. (2003) Structural, chemical and isotopic microanalytical investigations of graphite from supernovae. Geochimica et Cosmochimica Acta, 67, 4705–4725.
Croat, T.K., Stadermann, F.J., and Bernatowicz, T.J. (2005) Presolar graphite from AGB stars: Microsctructure and s-process enrichment. The Astrophysical Journal, 631, 976–987.
Croat, T.K., Stadermann, F.J., and Bernatowicz, T.J. (2008) Correlated isotopic and microstructural studies of turbostratic presolar graphites from the Murchison meteorite. Meteoritics & Planetary Science, 43, 1497–1516.
Croat, T.K., Stadermann, F.J., and Bernatowicz, T.J. (2010) Unusual ^{29,30}Si-rich SiCs of massive star origin found within graphites from the Murchison meteorite. The Astronomical Journal, 139, 2159–2169.
Croat, T.K., Jadhav, M., Lebsack, E., and Bernatowicz, T.J. (2011) TiC and rutile within a supernova graphite. Meteoritics & Planetary Science, 46, A51.
Croat, T.K., Berg, T., Bernatowicz, T.J., and Jadhav, M. (2013) Refractory metal nuggets within presolar graphite: First condensates from a circumstellar environment. Meteoritics & Planetary Science, 48, 686–699.
Dai, Z.R., Bradely, J.P., Joswiak, D.J., Brownlee, D.E., Hill, H.G.M., and Genge, M.J. (2002) Possible in situ formation of meteoritic nanodiamonds in the early solar system. Nature, 418, 157–159.
Dana, E.S. and Ford, W.E. (1947) Dana's Textbook of Mineralogy, 4th ed. Wiley.
Dana, J.D. (1850) A System of Mineralogy, Comprising the Most Recent Discoveries, Including Full Descriptions of Species and their Localities, Chemical Analyses and Formulas, Tables for the Determination of Minerals, and a Treatise on Mathematical Crystallography and the Drafting of Figures of Crystals, 3rd ed., Rewritten, Rearranged, and Enlarged. George P. Putnam.
Dana, J.D., Dana, E.S., Palache, C., Berman, H., and Frondel, C. (1973) Dana's System of Mineralogy, 7th ed., complete in 3 volumes. Wiley.
Daulton, T.L., Eisenhour, D.D., Bernatowicz, T.J., Lewis, R.S., and Buseck, P.R. (1996) Genesis of presolar diamonds: Comparative high-resolution transmission electron microscopy study of meteoritic and terrestrial nano-diamonds. Geochimica et Cosmochimica Acta, 60, 4853–4872.
Daulton, T.L., Bernatowicz, T.J., Lewis, R.S., Messenger, S., Stadermann, F.J., and Amari, S. (2002) Polytype distribution in circumstellar silicon carbide. Science, 296, 1852–1855.
Daulton, T.L., Bernatowicz, T.J., Lewis, R.S., Messenger, S., Stadermann, F.J., and Amari, S. (2003) Polytype distribution in circumstellar silicon carbide: Microstructural characterization by transmission electron microscopy. Geochimica et Cosmochimica Acta, 67, 4743–4767.
Davidson, J., Busemann, H., Nittler, L.R., Alexander, C.M.O'D., Orthous-Daunay, F.-R., Franchi, I.A., and Hoppe, P. (2014) Abundances of presolar silicon carbide grains in primitive meteorites determined by nanoSIMS. Geochimica et Cosmochimica Acta, 139, 248–266.
Davis, A.M. (2011) Stardust in meteorites. Proceedings of the National Academy of Sciences, 108, 19142–19146.
——— (2014) Meteorites and Cosmochemical Processes: Treatise on Geochemistry, vol. 1, 2nd ed. Elsevier-Pergamon.
Demyk, K., Dartois, E., Wiesemeyer, H., Jones, A.P., and d'Hendecourt, L. (2000) Structure and chemical composition of the silicate dust around OH/IR stars. Astronomy & Astrophysics, 364, 170–178.
DePew, K., Speck, A., and Dijkstra, C. (2006) Astromineralogy of the 13 micrometer feature in the spectra of oxygen-rich asymptotic giant branch stars. I. corundum and spinel. The Astrophysical Journal, 640, 971–981.
Dermott, S.F. and Liou, J.C. (1994) Detection of asteroidal dust particles from known families in near-Earth orbits. In M. Zolensky, T. Wilson, F. Rietmeijer, and G. Flynn, Eds., Analysis of Interplanetary Dust, pp.13–22. American Institute of Physics.
Ebel, D.S. (2006) Condensation of rocky materials in astrophysical environments. In D.S. Lauretta and H.Y. McSween Jr., Eds., Meteorites and the Early Solar System II, pp. 253–277. University of Arizona Press, Tucson.
Ebel, D.S., and Grossman, L. (2000) Condensation in dust-rich systems. Geochimica et Cosmochimica Acta, 65, p. 469–477.
Everitt, B. (2011) Cluster Analysis. Wiley.
Fahey, A.J., Goswami, J.N., McKeegan, K.D., and Zinner, E. (1987) ^{26}Al, ^{244}Pu, ^{50}Ti, REE and trace element abundances in hibonite grains from CM and CV meteorites. Geochimica et Cosmochimica Acta, 51, 329–350.
Feigelson, E.D., Broos, P., Gaffney, J.A. III, Garmire, G., Hillenbrand, L.A., Pravdo, S.H., Townsley, L., and Tsuboi, Y. (2002) X-ray emitting young stars in the Orion Nebula. The Astrophysical Journal, 574, 258–292.
Feltzing, S., and Gonzales, G. (2001) The nature of super-metal-rich stars. Detailed abundance analysis of 8 super metal-rich star candidates. Astronomy & Astrophysics, 367, 253–265.
Floss, C., and Stadermann, F. (2009) Auger Nanoprobe analysis of presolar ferromagnesian silicate grains from primitive CR chondrites QUE 99177 and MET 00426. Geochimica et Cosmochimica Acta, 73, 2415–2440.
——— (2012) Presolar silicate and oxide abundances and compositions in the ungrouped carbonaceous chondrite Adelaide and the K chondrite Kakangari: The effects of secondary processing. Meteoritics & Planetary Science, 47, 992–1009.
Floss, C., Stadermann, F.J., and Bose, M. (2008) Circumstellar Fe oxide from the Acfer 094 carbonaceous chondrite. The Astrophysical Journal, 672, 1266–1271.
Forrest, W.J., Gillett, F.C., and Stein, W.A. (1975) Circumstellar grains and the intrinsic polarization of starlight. The Astrophysical Journal, 195, 423–440.
Fraundorf, P., and Wackenhut, M. (2002) The core structure of presolar graphite onions. The Astrophysical Journal Letters, 578, L153–L156.
Frebel, A., Johnson, J.L., and Bromm, V. (2009) The minimum stellar metallicity observable in the Galaxy. Monthly Notices of the Royal Astronomical Society, 392, L50–L54.
Fujiya, W., Hoppe, P., Zinner, E., Pignatari, M., and Herwig, F. (2013) Evidence for radiogeneic sulfur-32 in type AB presolar silicon carbide grains? The Astrophysical Journal Letters, 776, L29 (6 pp).
Gaines, R.V., Skinner, H.C.W., Foord, E.E., Mason, B., and Rosenzweig, A. (1997) Dana's New Mineralogy: The System of Mineralogy of James Dwight Dana and Edward Salisbury Dana, 8th ed. Wiley.
Ghirlanda, G., Salafia, O.S., Paragi, Z., Giroletti, M., and 32 others (2019) Compact radio emission indicates a structured jet was produced by a binary neutron star merger. Science, 363, 968–971.
Gillett, F.C., Low, F.J., and Stein, W.A. (1968) Stellar spectra from 2.8 to 14 microns. The Astrophysical Journal, 154, 677.
Gobrecht, D., Cherchneff, I., Sarang, A., Piene, J.M.C., and Bromley, S.T. (2016) Dust formation in the oxygen-rich AGB star 1K Tauri. Astronomy & Astrophysics, 585, Article A6, 15 p.
Grew, E.S., Dymek, R.F., De Hoog, J.C.M., Harley, S.L., Boak, J.M., Hazen, R.M., and Yates, M.G. (2015) Boron isotopes in tourmaline from the 3.7–3.8 Ga Isua Belt, Greenland: Sources for boron in Eoarchean continental crust and seawater. Geochimica et Cosmochimica Acta, 163, 156–177.
Groopman, E., and Nittler, L.R. (2018) Correlated XANES, TEM, and NanoSIMS of presolar graphite grains. Geochimica et Cosmochimica Acta, 221, 219–236.
Groopman, E., Bernatowicz, T., and Zinner, E. (2012) C, N, and O isotopic heterogeneities in low-density supernova graphite grains from Orgueil. The Astrophysical Journal Letters, 754, L8 (6 pp).
Grossman, L. (1972) Condensation in the primitive solar nebula. Geochimica et Cosmochimica Acta, 36, 597–619.
Gyngard, F., Amari, S., Zinner, E., and Ott, U. (2009) Interstellar exposure age of large presolar SiC grains from the Murchison meteorite. The Astrophysical Journal, 694, 359–366.
Gyngard, F., Zinner, E., Nittler, L.R., Morgand, A., Stadermann, F.J., and Hynes, K.M. (2010a) Automated nanoSIMS measurements of spinel stardust from the Murray meteorite. The Astrophysical Journal, 717, 107–120.
Gyngard, F., Nittler, L.R., and Zinner, E. (2010b) Presolar SiC grains of Type C. Meteoritics & Planetary Sciences, 45, A72.
Gyngard, F., Nittler, L.R., Zinner, E., José, J., and Cristallo, S. (2011) New reaction rates and implications for nova nucleosynthesis and presolar grains. Lunar and Planetary Science, 42, #2675.
Gyngard, F., Jadhav, M., Nittler, L.R., Stroud, R.M., and Zinner, E. (2018) Bonanza: An extremely large dust grain from a supernova. Geochimica et Cosmochimica Acta, 221, 60–86.
Haenecour, P., Floss, C., Jose, J., Amari, S., Lodders, K., Jadhav, M., Wang, A., and Gyngard, F. (2016) Coordinated analysis of two graphite grains from the CO3.0 LAP031117 meteorite: First identification of a CO nova graphite and a presolar iron sulfide subgrain. The Astrophysical Journal, 825, 88 (9 pp).
Han, J., Brearley, A.J., and Keller, L.P. (2015) Microstructural evidence for a disequilibrium condensation origin for hibonite-spinel inclusions in the ALHA77307 CO3.0 chondrite. Meteoritics & Planetary Science, 50, 2121–2136.
Hazen, R.M. (1984) Mineralogy: A historical review. Journal of Geological Education, 32, 288–298.
——— (2019) An evolutionary system of mineralogy: Proposal for a classification of planetary materials based on natural kind clustering. American Mineralogist, 104, 810–816.
Hazen, R.M., and Ferry, J.M. (2010) Mineral evolution: Mineralogy in the fourth dimension. Elements, 6, 9–12.
Hazen, R.M., Papineau, D., Bleeker, W., Downs, R.T., Ferry, J.M., McCoy, T.L., Sverjensky, D.A., and Yang, H. (2008) Mineral evolution. American Mineralogist, 93, 1693–1720.
Hazen, R.M., Hystad, G., Downs, R.T., Golden, J.J., Pires, A.J., and Grew, E.S. (2015) Earth's "missing" minerals. American Mineralogist, 100, 2344–2347.
Heck, P.R., Amari, S., Hoppe, P., Baur, H., Lewis, R.S., and Wieler, R. (2009a) Ne isotopes in individual presolar graphite grains from the Murchison meteorite together with He, C, O, Mg-Al isotopic analyses as tracers of their origins. The Astrophysical Journal, 701, 1415–1425.
Heck, P.R., Gyngard, F., Ott, U., Meier, M.M.M., Ávila, J.N., Amari, S., Zinner, E.K., Lewis, R., Baur, H., and Wieler, R. (2009b) Interstellar residence times of presolar SiC dust grains from the Murchison carbonaceous chondrite. The Astrophysical

Journal, 698, 1155–1173.
Heck, P.R., Stadermann, F.J., Isheim, D., Auciello, O., Daulton, T.L., Davis, A.M., Elam, J.W., Floss, C., Hiller, J., Larson, D.J., Lewis, J.B., Mane, A., Pellin, M.J., Savina, M.R., Seidman, D.N., and Stephan, T. (2014) Atom-probe analyses of nanodiamonds from Allende. Meteoritics & Planetary Science, 49, 453–467.
Herwig, F., Pignatari, M., Woodward, P.R., Porter, D.H., Rockefeller, G., Fryer, C.L., Bennett, M., and Hirschi, R. (2011) Convective-reactive proton-^{12}C combustion in Sakurai's object (V4334 Sagittarii) and implications for the evolution and yields from the first generations of stars. The Astrophysical Journal, 727, 89–111.
Hinton, R.W., Davis, A.M., Scatena-Wachel, D.E., Grossman, L., and Draus, R.J. (1988) A chemical and isotopic study of hibonite-rich refractory inclusions in primitive meteorites. Geochimica et Cosmochimica Acta, 52, 2573–2598.
Hodge, P.W. (1961) Sampling dust from the stratosphere. Smithsonian Contributions to Astrophysics, 5, 145–152.
Höfner, S. (2008) Winds of M-type AGB stars driven by micron-sized grains. Astronomy & Astrophysics, 491, L1–L4.
Hohenberg, C.M., Nichols, R.H. Jr., Olinger, C.T., and Goswami, J.N. (1990) Cosmogenic neon from individual grains of CM meteorites: Extremely long pre-compaction exposure histories or an enhanced early particle flux. Geochimica et Cosmochimica Acta, 54, 2133–2140.
Hong, Y., and Fegley, B. Jr. (1998) Experimental studies of magnetite formation in the solar system. Meteoritics & Planetary Science, 33, 1101–1112.
Hoppe, P., Amari, S., Zinner, E., Ireland, T., and Lewis, R.S. (1994) Carbon, nitrogen, magnesium, silicon, and titanium isotopic compositions of single interstellar silicon carbide grains from the Murchison meteorite. The Astrophysical Journal, 430, 870–890.
Hoppe, P., Amari, S., Zinner, E., and Lewis, R.S. (1995) Isotopic compositions of C, N, O, Mg, and Si, trace element abundances, and morphologies of single circumstellar graphite grains in four density fractions from the Murchison meteorite. Geochimica et Cosmochimica Acta, 59, 4029–4056.
Hoppe, P., Strebel, R., Eberhardt, P., Amari, S., and Lewis, R.S. (1996) Small SiC grains and a nitride grain of circumstellar origin from the Murchison carbonaceous chondrite. Geochimica et Cosmochimica Acta, 60, 883–907.
Hoppe, P., Annen, P., Strebel, R., Eberhardt, P., Gallino, R., Lugaro, M., Amari, S., and Lewis, R.S. (1997) Meteoritic silicon carbide grains with unusual Si-isotopic compositions: Evidence for an origin in low-mass, low-metallicity asymptotic giant branch stars. The Astrophysical Journal, 487, L101–L104.
Hoppe, P., Strebel, R., Eberhardt, P., Amari, S., and Lewis, R.S. (2000) Isotopic properties of silicon carbide X grains from the Murchison meteorite in the size range 0.5–1.5 microns. Meteoritics & Planetary Sciences, 35, 1157–1176.
Hoppe, P., Leitner, J., Gröner, E., Marhas, K.K., Meyer, B.S., and Amari, S. (2010) NanoSIMS isotopic analysis of small presolar SiC grains: New insights into supernova nucleosynthesis, chemistry, and dust formation. The Astrophysical Journal, 719, 1370–1384.
Huss, G.R., Fahey, A.J., Galilino, R., and Wasserburg, G.J. (1994) Oxygen isotopes in circumstellar Al_2O_3 grains from meteorites and stellar nucleosynthesis. The Astrophysical Journal Letters, 430, L81–L84.
Huss, G.R., Hutcheon, I.D., and Wasserburg, G.J. (1997) Isotopic systematics of presolar silicon carbide from the Orgueil (CI) carbonaceous chondrite: Implications for solar system formation and stellar nucleosynthesis. Geochimica et Cosmochimica Acta, 61, 5117–5148.
Hutcheon, I.D., Huss, G.R., Fahey, A.J., and Wasserburg, G.J. (1994) Extreme ^{26}Mg and ^{17}O enrichments in an Orgueil corundum: Identification of a presolar oxide grain. The Astrophysical Journal Letters, 425, L97–L100.
Hynes, K.M. (2010) Microanalytical investigations of presolar SiC grains as probes of condensation conditions in astrophysical environments. Ph.D. thesis, Washington University, St. Louis, Missouri.
Hynes, K.M., and Gyngard, F. (2009) The presolar grain database. Lunar and Planetary Science Conference, 42, #1595.
Hynes, K.M., Croat, T.K., Amari, S., Mertz, A.F., and Bernatowicz, T.J. (2010) Structural and isotopic microanalysis of presolar SiC from supernovae. Meteoritics & Planetary Sciences, 45, 596–614.
Hynes, K.M., Amari, S., Bernatowicz, T.J., Lebsack, E., Gyngard, F., and Nittler, L.R. (2011) Combined TEM and NanoSIMS analysis of subgrains in a SiC AB grain. Lunar and Planetary Science, 42, #2332.
Iliadis, C., Downen, L.N., Jose, J., Nittler, L.R., and Starrfield, S. (2018) On presolar stardust grains from CO classical novae. The Astrophysical Journal, 855, 76 (14 pp).
Iocco, F., Mangano, G., Miele, G., Pisanti, O., and Serpico, P.D. (2008) Primordial nucleosynthesis: from precision cosmology to fundamental physics. Physics Reports, 472, 1–76.
Ireland, T.R. (1988) Correlated morphological, chemical, and isotopic characteristics of hibonites from the Murchison carbonaceous chondrite. Geochimica et Cosmochimica Acta, 52, 2827–2839.
——— (1990) Presolar isotopic and chemical signatures in hibonite-bearing refractory inclusions from the Murchison carbonaceous chondrite. Geochimica et Cosmochimica Acta, 54, 3219–3237.
Jadhav, M., Amari, S., Marhas, K.K., Zinner, E., Maruoka, T., and Gallino, R. (2008) New stellar sources for high-density, presolar graphite grains. The Astrophysical Journal, 682, 1479–1485.
Jadhav, M., Zinner, E., Amari, S., Maruoka, T., Marhas, K.K., and Gallino, R. (2013) Multi-element isotopic analyses of presolar graphite grains from Orgueil. Geochimica et Cosmochimica Acta, 113, 193–224.
Jiang, B.W., Zhang, K., Li, A., and Lisse, C.M. (2013) Crystalline silicates in evolved stars. I. Spitzer/infrared spectrograph spectroscopy of IRAS 16456-3542, 18354-0638, and 23239+5754. The Astrophysical Journal, 765, 72 (7 pp).
Johnson, J.A. (2019) Populating the periodic table: nucleosynthesis of the elements. Science, 363, 474–478.
Jones, A.P. (2007) The mineralogy of cosmic dust: astromineralogy. European Journal of Mineralogy, 19, 771–782.
Jones, A.P., Tielens, A.G.G.M., Hollenbach, D.J., and McKee, C.F. (1994) Grain destruction in shocks in the interstellar medium. The Astrophysical Journal, 433, 797–810.
Jones, L.V. (2009) Stars and Galaxies. ABC-CLIO.
Jones, T.W., and Merrill, K.M. (1976) Model dust envelopes around late-type stars. The Astrophysical Journal, 209, 509–524.
Jones, O.C., Kemper, F. Sargent, B.A., McDonald, I., Gielen, C., Woods, P.M., Sloan, G.C., Boyer, M.L., Zijlstra, A.A., Clayton, G.C., and others. (2012) On the metallicity dependence of crystalline silicates in oxygen-rich asymptotic giant branch stars and red supergiants. Monthly Notices of the Royal Astronomical Society, 427, 3209–3229.
Jones, S., Côte, B., Röpke, F.K., and Wanajo, S. (2019a) A new model for electron-capture supernovae in galactic chemical evolution. The Astrophysical Journal, 882, 170–179.
Jones, S., Röpke, F.K., Freyer, C., Ruiter, A.J., Seitenzahl, I.R., Nittler, L.R., Ohlmann, S.T., Reifarth, R., Pignatari, M., and Belczynski, K. (2019b) Remnants and ejecta of thermonuclear electron-capture supernovae: Constraining oxygen-neon deflagrations in high-density white dwarfs. Astronomy & Astrophysics, 622, A74 (22 p.).
José, J., and Hernandez, M. (2007) The origin of presolar nova grains. Meteoritics & Planetary Science, 42, 1135–1143.
Käppeler, F. (1999) The origin of the heavy elements: the *s* process. Progress in Particle and Nuclear Physics, 43, 419–483.
Karakas, A.I., and Lattanzio, J.C. (2014) The Dawes Review 2: Nucleosynthesis and the stellar yields of low and intermediate-mass single stars. Publications of the Astronomical Society of Australia, 31, e030.
Karttunen, H., and Oja, H. (2007) Fundamental Astronomy, 5th edition. Springer.
Kasen, D., Metzger, B., Barnes, J., Quataert, E., and Ramirez-Ruiz, E. (2017) Origin of the heavy elements in binary neutron star mergers from a gravitational-wave event. Nature, 551, 80–84.
Kelly, J.F., Fisher, G.R., and Barnes, P. (2005) Correlation between layer thickness and periodicity of long polytypes in silicon carbide. Materials Research Bulletin, 40, 249–255.
Kemper, F., Vriend, W.J., and Tielens, A.G.G.M. (2004) The absence of crystalline silicates in the diffuse interstellar medium. The Astrophysical Journal, 609, 826–837.
Kemper, F., Markwick, A.J., and Woods, P.M. (2011) The crystalline fraction of interstellar silicates in starburst galaxies. Monthly Notices of the Royal Astronomical Society, 413, 1192–1199.
Khokhlov, A. Müller, E., and Höflich, P. (1993) Light curves of Type 1a supernova models with different explosion mechanisms. Astronomy & Astrophysics, 270, 223–248.
Kööp, L., Heck, P.R., Busemann, H., Davis, A.M., Greer, J., Maden, C., Meier, M.M.M., and Wieler, R. (2018) High early solar activity inferred from helium and neon excesses in the oldest meteorite inclusions. Nature Astronomy, 2, 709–713.
Lauretta, D.S., Lodders, K., and Fegley, B. Jr. (1998) Kamacite sulfurization in the solar nebula. Meteoritics & Planetary Science, 33, 821–834.
Leitner, J., Vollmer, C., Hoppe, P., and Zipfel, J. (2012a) Characterization of presolar material in the CR chondrite Northwest Africa 852. The Astrophysical Journal, 745, 38–52.
Leitner, J., Kodolányi, J., Hoppe, P., and Floss, C. (2012b) Laboratory analysis of presolar silicate stardust from a nova. The Astrophysical Journal Letters, 754, L41.
Leitner, J., Hoppe, P., Floss, C., Hillion, F., and Henkel, T. (2018) Correlated nanoscale characterization of a unique complex oxygen-rich stardust grain: Implications for circumstellar dust formation. Geochimica et Cosmochimica Acta, 221, 255–274.
Lewis, R.S., Ming, T., Wacker, J.F., Anders, E., and Steel, E. (1987) Interstellar diamonds in meteorites. Nature, 339, 117–121.
Lewis, R.S., Amari, S., and Anders, E. (1990) Meteoritic silicon carbide: Pristine material from carbon stars. Nature, 348, 293–298.
Lewis, R.S., Amari, S., and Anders, E. (1994) Interstellar grains in metorites: II. SiC and its noble gases. Geochimica et Cosmochimica Acta, 58, 471–494.
Lewis, J.B., Floss, C., and Gyngard, F. (2018) Origin of nanodiamonds from Allende constrained by statistical analysis of C isotopes from small clusters of acid residue by NanoSIMS. Geochimica et Cosmochimica Acta, 221, 237–254.
Limongi, M., and Chieffi, A. (2012) Evolution, explosion, and nucleosynthesis of core-collapse supernovae. The Astrophysical Journal Supplement Series, 199, 38–46.
Lin, Y., Gyngard, F., Zinner, E. (2010) Isotopic analysis of supernova SiC and Si_3N_4 grains from the Qingzhen (EH3) chondrite. The Astrophysical Journal, 709, 1157–1173.
Little-Marenin, I.R., and Little, S.J. (1990) Emission features in IRAS low-resolution spectra of MS,S and SC stars. The Astrophysical Journal, 333, 305–315.
Liu, N., Nittler, L.R., Alexander, C.M.O'D., Wang, J., Pignatari, M., José, J., and Nguyen, A.N. (2016) Stellar origins of extremely ^{13}C- and ^{15}N-enriched presolar SiC grains: Novae or supernovae? The Astrophysical Journal, 820, 140 (14 pp).
Liu, N., Stephan, T., Boehnke, P., Nittler, L.R., Alexander, C.M.O'D., Wang, J., Davis, A.M., Trappitsch, R., and Pellin, M.J. (2017a) J-type carbon stars: A dominant source of ^{14}N-rich presolar SiC grains of type AB. The Astrophysical Journal

Letters, 844, L12.
Liu, N., Steele, A., Nittler, L.R., Stroud, R.M, De Gregorio, B.T., Alexander, C.M.O'D., and Wang, J. (2017b) Coordinated EDX and micro-Raman analysis of presolar silicon carbide: A novel, nondestructive method to identify rare subgroup SiC. Meteoritics & Planetary Science, 52, 1–20.
Liu, N., Nittler, L.R., Pignatari, M., Alexander, C.M.O'D., and Wang, J. (2017c) Stellar origin of ^{15}N-rich presolar SiC grains of Type AB: Supernovae with explosive hydrogen burning. Astrophysical Journal Letters, 842, L1.
Liu, N., Nittler, L.R., Alexander, C.M.O'D., and Wang, J. (2018) Late formation of silicon carbide in type II supernovae. Science Advances, 4, eaao1054.
Lodders, K. (2003) Solar system abundance and condensation temperatures of the elements. The Astrophysical Journal, 591, 1220–1247.
Lodders, K., and Amari, S. (2005) Presolar grains from meteorites: Remnants from the early times of the solar system. Chemie der Erde, 65, 93–166.
Lugaro, M. (2005) Stardust from Meteorites: An Introduction to Presolar Grains. World Scientific.
Lugaro, M., Zinner, E., Gallino, R., and Amari, S. (1999) Isotopic ratios in mainstream presolar SiC grains revisited. The Astrophysical Journal, 527, 369–394.
Lugaro, M., Karakas, A.I., Bruno, C.G., Aliotta, M., Nittler, L.R., and 32 others (2017) Origin of meteoritic stardust unveiled by a revised proton-capture rate of ^{17}O. Nature Astronomy, 1, 0027.
Ma, C., Krot, A.N., and Bizzarro, M. (2013) Discovery of dmisteinbergite (hexagonal $CaAl_2Si_2O_8$) in the Allende meteorite: A new member of refractory silicates formed in the solar nebula. American Mineralogist, 98, 1368–1371.
Ma, C., Krot, A.N., and Nagashima, K. (2017) Addibischoffite, $CaAl_6Al_6O_{20}$, a new calcium aluminate mineral from the Acfer 214 CH carbonaceous chondrite: A new refractory phase from the solar nebula. American Mineralogist, 102, 1556–1560.
Matteucci, F. (2003) The Chemical Evolution of the Galaxy. Kluwer Academic.
Mazzali, P.A., Röpke, F.K., Benetti, S., and Hillebrandt, W. (2007) A common explosion mechanism for type 1a supernovae. Science, 315, 825–828.
McAdam, M.M., Sunshine, J.M., Howard, K.T., Alexander, C.M.O'D., McCoy, T.J., and Bus, S.J. (2018) Spectral evidence for amorphous silicates in least-processed CO meteorites and their parent bodies. Icarus, 306, 32–49.
McKeegan, K.D., Aleon, J., Bradley, J., Brownlee, D., Busemann, H., Butterworth, A., Chaussidon, M., Fallon, S., and 39 others (2006) Isotopic compositions of cometary matter returned by Stardust. Science, 314, 1724–1728.
Meier, M.M.M., Heck, P.R., Amari, S., Baur, H., and Wieler, R. (2012) Graphite grains in supernova ejecta—Insights from a noble gas study of 91 individual KFC1 presolar graphite grains from the Murchison meteorite. Geochimica et Cosmochimica Acta, 76, 147–160.
Messenger, S. (2002) Opportunities for the stratospheric collection of dust from short-period comets. Meteoritics & Planetary Science, 37, 1491–1505.
Messenger, S., Keller, L.P., Stadermann, F.J., Walker, R.M., and Zinner, E. (2003) Samples of stars beyond the solar system: Silicate grains in interplanetary dust. Science, 300, 105–108.
Messenger, S., Keller, L.P., and Lauretta, D.S. (2005) Supernova olivine from cometary dust. Science, 309, 737–741.
Meyer, B.S., Clayton, D.D., and The, L.-S. (2000) Molybdenum and zirconium isotopes from a supernova neutron burst. The Astrophysical Journal, 540, L49–L52.
Millikan, R.G. (1999) Historical kinds and the special sciences. Philosophical Studies, 95, 45–65.
Mills, S.J., Hatert, F., Nickel, E.H., and Ferrais, G. (2009) The standardization of mineral group hierarchies: Application to recent nomenclature proposals. European Journal of Mineralogy, 21, 1073–1080.
Morgan, D.H., Cannon, R.D., Hatzidimitriou, D., and Croke, B.F.W. (2003) J-type carbon stars in the Large Magellanic Cloud. Monthly Notices of the Royal Astronomical Society, 341, 534–550.
Morrison, S.M., Liu, C., Eleish, A., Prabhu, A., Li, C., Ralph, J., Downs, R.T., Golden, J.J., Fox, P., and Hazen, R.M. (2017) Network analysis of mineralogical systems. American Mineralogist, 102, 1588–1596.
Mostefouai, S., and Hoppe, P. (2004) Discovery of abundant in situ silicate and spinel grains from red giant stars in a primitive meteorite. The Astrophysical Journal, 613, L149–L152.
Nagashima, K., Krot, A.N., and Yurimoto, H. (2004) Stardust silicates from primitive meteorites, Nature, 428, 921–924.
Neugebauer, G., Habing, H.J., van Duinen, R., Aumann, H.H., Baud, B., Beichman, C.A., Beintema, D.A., Boggess, N., Clegg, P.E., de Jong, T., and others. (1984) The Infrared Astronomical Satellite (IRAS) mission. The Astrophysical Journal, Part 2, 278, L1–L6.
Nguyen, A.N. and Messenger, S. (2014) Resolving the stellar sources of isotopically rare presolar silicate grains through Mg and Fe isotopic analysis. The Astrophysical Journal, 784, 149 (15 pp).
Nguyen, A.N., and Zinner, E. (2004) Discovery of ancient silicate stardust in a meteorite. Science, 303, 1496–1499.
Nguyen, A.N., Stadermann, F.J., Zinner, E., Srtroud, R.M., Alexander, C.M.O'D., and Nittler, L.R. (2007) Characterization of presolar silicate and oxide grains in primitive carbonaceous chondrites. The Astrophysical Journal, 656, 1223–1240.
Nguyen, A.N., Nittler, L.R., Stadermann, F.J., Stroud, R.M., and Alexander, C.M.O'D. (2010) Coordinated analyses of presolar grains in the Allan Hills 77307 and Queen Elizabeth Range 99177 meteorites. The Astrophysical Journal, 719, 166–189.
Nguyen, A.N., Keller, L.P., and Messenger, S. (2016) Mineralogy of presolar silicate and oxide grains of diverse stellar origins. The Astrophysical Journal, 818, 51 (17 pp).
Nguyen, A.N., Nittler, L.R., Alexander, C.M.O'D., and Hoppe, P. (2018) Titanium isotopic compositions of rare presolar SiC grain types from the Murchison meteorite. Geochimica et Cosmochimica Acta, 221, 162–181.
Nittler, L.R., and Alexander, C.M.O'D. (2003) Automated isotopic measurements of micron-sized dust: Application to meteoritic presolar silicon carbide. Geochimica et Cosmochimica Acta, 67, 4961–4980.
Nittler, L.R., and Ciesla, F. (2016) Astrophysics with extraterrestrial materials. Annual Review of Astronomy & Astrophysics, 54, 53–93.
Nittler, L.R. and Dauphas, N. (2006) Meteorites and the chemical evolution of the Milky Way. In D.S. Lauretta and H.Y. McSween Jr., Eds., Meteorites and the Early Solar System II, pp.127–146. University of Arizona Press.
Nittler, L.R., Alexander, C.M.O'D., Gao, X., Walker, R.M., and Zinner, E. (1994) Interstellar oxide grains from the Tieschitz ordinary chondrite. Nature, 370, 443–446.
Nittler, L.R., Hoppe, P., Alexander, C.M.O'D., Amari, S., Eberhardt, P., Gao, X., Lewis, R.S., Strebel, R., Walker, R.M., and Zinner, E. (1995) Silicon nitride from supernovae. The Astrophysical Journal, 453, L25–L28.
Nittler, L.R., Amari, S., Zinner, E., Woosley, S.E., and Lewis, R.S. (1996) Extinct ^{44}Ti in presolar graphite and SiC: Proof of a supernova origin. The Astrophysical Journal Letters, 462, L31–L34.
Nittler, L.R., Alexander, C.M.O'D., Gao, X., Walker, R.M., and Zinner, E. (1997) Stellar sapphires: The properties and origins of presolar Al_2O_3 in meteorites. The Astrophysical Journal, 483, 475–495.
Nittler, L.R., Alexander, C.M.O'D., Stadermann, F.J., and Zinner, E.K. (2005) Presolar chromite in Orgueil. Meteoritics & Planetary Science, 40, A114.
Nittler, L.R., Alexander, C.M.O'D., Gallino, R., Hoppe, P., Nguyen, A.N., Stadermann, F.J., and Zinner, E.K. (2008) Aluminum-, calcium-, and titanium-rich oxide stardust in ordinary chondrite meteorites. The Astrophysical Journal, 682, 1450–1478.
Nittler, L.R., Gyngard, F., Zinner, E., and Stroud, R.M. (2011) Mg and Ca isotopic anomalies in presolar oxides: Large anomalies in a group 3 hibonite grain. Lunar and Planetary Science, 42, #1872.
Nittler, L.R., Alexander, C.M.O'D., Liu, N., and Wang, J. (2018a) Extremely ^{54}Cr- and ^{50}Ti-rich presolar oxide grains in a primitive meteorite: Formation in rare types of supernovae and implications for the astrophysical context of Solar System birth. The Astrophysical Journal Letters, 856, L24 (7 pp).
Nittler, L.R., Alexander, C.M.O'D., Davidson, J., Riebe, M.E.I., Stroud, R.M., and Wang, J. (2018b) High abundances of presolar grains and ^{15}N-rich organic matter in CO3.0 chondrite Dominion Range 08006. Geochimica et Cosmochimica Acta, 226, 107–131.
Nollett, K.M., Busso, M., and Wasserburg, G.J. (2003) Cool bottom processing on the thermally pulsing asymptotic giant branch and the isotopic composition of circumstellar dust grains. The Astrophysical Journal, 582, 1036–1058.
Nuth, J.A. III, and Allen, J.E. Jr. (1992) Supernovae as sources of interstellar diamonds. Astrophysics and Space Science, 196, 117–123.
Onaka, T., de Jong, T., and Willems, F.J. (1989) A study of M Mira variables based on IRAS LRS observations. I—dust formation in the circumstellar shell. Astronomy & Astrophysics, 18, 169–179.
Ozima, M., and Mochizuki, K. (1993) Origin of nanodiamonds in primitive chondrites: (1) Theory. Meteoritics, 28, 416–417.
Pagel, B.E.J. (1997) Nucleosynthesis and Chemical Evolution of Galaxies. Cambridge University Press.
Peeples, M.S., and Somerville, R.S. (2013) An empirical prediction for stellar metallicity distributions in nearby galaxies. Monthly Notices of the Royal Astronomical Society, 428, 1766–1773.
Prialnik, D. (2001) Novae. In P. Murdin, Ed., Encyclopedia of Astronomy and Astrophysics, pp. 1846–1856. Institute of Physics Publishing, Washington, D.C.
Rauscher, T., Heger, A., Hoffman, R.D., and Woosley, S.E. (2002) Nucleosynthesis in massive stars with improved nuclear and stellar physics. The Astrophysical Journal, 576, 323–348.
Rieke, G.H. (2009) History of infrared telescopes and astronomy. Experimental Astronomy, 25, 125–141.
Richter, S., Ort, U., and Begemann, F. (1998) Tellurium in pre-solar diamonds as an indicator of rapid separation of supernova ejecta. Nature, 391, 261–263.
Robertson, B.E., Ellis, R.S., Furlanetto, S.R., and Dunlop, J.S. (2015) Cosmic reionization and early star-forming galaxies: A joint analysis of new constraints from Planck and the Hubble Space Telescope. The Astrophysical Journal, 802, L19–L23.
Rolfs, C.E., and Rodney, W.S. (2005) Cauldrons in the Cosmos: Nuclear Astrophysics. University of Chicago Press.
Rubin, A.E., and Ma, C. (2017) Meteoritic minerals and their origins. Chemie der Erde, 77, 325–385.
Russell, S.S., Arden, J.W., and Pillinger, C.T. (1991) Evidence for multiple sources of diamond from primitive chondrites. Science, 254, 1188–1191.
——— (1996) A carbon and nitrogen isotope study of diamond from primitive chondrites. Meteoritics & Planetary Science, 31, 343–355.
Salpeter, E.E. (1977) Formation and destruction of dust grains. Annual Review of Astronomy & Astrophysics, 15, 267–293.
Santana, C. (2019) Mineral misbehavior: why mineralogists don't deal in natural kinds. Frontiers of Chemistry, https//doi.org/10.1007/s10698-019-09338-3.
Sarangi, A., and Cherchneff, I. (2015) Condensation of dust in the ejecta of Type II

supernovae. Astronomy & Astrophysics, 575, A95 (20 pp).
Schatz, H. (2010) The evolution of elements and isotopes. Elements, 6, 13–17.
Schertl, H.-P., Mills, S.J., and Maresch, W.V. (2018) A Compendium of IMA-Approved Mineral Nomenclature. International Mineralogical Association, Melbourne, Australia.
Schröder, K.-P., and Connon Smith, R. (2008) Distant future of the Sun and Earth revisited. Monthly Notices of the Royal Astronomical Society, 386, 155–163.
Sloan, G.C., and Price, S.D. (1998) The infrared spectral classification of oxygen-rich dust shells. The Astrophysical Journal Supplement Series, 119, 141–158.
Sloan, G.C., Kraemer, K.E., McDonald, I., Groenewegen, M.A.T., Wood, P.R., Zijlstra, A.A., Lagadec, E., Boyer, M.L., Kemper, F., Matsuura, M., Sahai, R., Sargent, B.A., Srinivasan, S., van Loon, J.T., and Volk, K. (2016) The infrared spectral properties of Magellanic carbon stars. The Astrophysical Journal, 826, 44 (19 pp).
Sneden, C., Cowan, J.J., and Gallino, R. (2008) Neutron-capture elements in the early galaxy. Annual Review of Astronomy & Astrophysics, 46, 241–288.
Soker, N., and Harpaz, A. (1999) Stellar structure and mass loss on the upper asymptotic giant branch. Monthly Notices of the Royal Astronomical Society, 310, 1158–1164.
Sossi, P.A., Moynier, F., Chaussidon, M., Villeneuve, J., Kato, C., and Gounelle, M. (2017) Early solar system irradiation quantified by linked vanadium and beryllium isotope variations in meteorites. Nature Astronomy, 1, article 55.
Speck, A.K., Barlow, M.J., Sylvester, R.J., and Hofmeister, A.M. (2000) Dust features in the 10-micrometer infrared spectra of oxygen-rich evolved stars. Astronomy & Astrophysics, 146, 437–464.
Stadermann, F.J., Croat, T.K., Bernatowiicz, T.J., Amario, S., Messenger, S., Walker, R.M., and Zinner, E. (2005) Supernova graphite in the NanoSIMS: Carbon, oxygen and titanium isotopic compositions of a spherule and its TiC sub-components. Geochimica et Cosmochimica Acta, 69, 177–188.
Stadermann, F.J., Hoppe, P., Floss, C., Heck, P.R., Hörz, F., Huth, J., Kearsley, A.T., Leitner, J., Marhas, K.K., McKeegan, K.D., and Stephan, T. (2008) Stardust in Stardust—The C, N, and O isotopic compositions of Wild 2 cometary matter in Al foil impacts. Meteoritics & Planetary Science, 43, 299–313.
Stein, W.A., Gaustad, J.E., Gillett, F.C., and Knacke, R.F. (1969) The spectrum of Cygnus from 7.5 to 14 microns. The Astrophysical Journal, 155, L177–L179.
Stroud, R.M., and Bernatowicz, T.J. (2005) Surface and internal structure of pristine presolar silicon carbide. Lunar and Planetary Science Conference, 36, #2010.
Stroud, R.M., Nittler, L.R., and Hoppe, P. (2004a) Microstructures and isotopic compositions of two SiC X grains. Meteoritics & Planetary Science, 39, A101.
Stroud, R.M., Nittler, L.R., and Alexander, C.M.O'D. (2004b) Polymorphism in presolar Al_2O_3: Grains from asymptotic giant branch stars. Science, 305, 1455–1457.
Stroud, R.M., Chisholm, M.F., Heck, P.R., Alexander, C.M.O'D., and Nittler, L.R. (2011) Supernova shock-wave-induced co-formation of glassy carbon and nanodiamond. The Astrophysical Journal, 738, L27 (5 pp).
Takigawa, A., Tachibana, S., Huss, G.R., Nagashima, K., Makide, K., Krot, A.N., and Nagahara, H. (2014) Morphology and crystal structures of solar and presolar Al_2O_3 in unequilibrated ordinary chindrites. Geochimica et Cosmochimica Acta, 124, 309–327.
Takigawa, A., Tachibana, S., Nagahara, H., and Ozawa, K. (2015) Evaporation and condensation kinetics of corundum: The origin of the 13-micrometer feature of oxygen-rich AGB stars. The Astrophysical Journal Supplement Series, 218, (16 pp). doi: 10.1088/0067-0049/218/1/2.
Takigawa, A., Stroud, R.M., Nittler, L.R., and Alexander, C.M.O'D. (2018) High-temperature dust condensation around an AGB star: evidence from a highly pristine presolar corundum. The Astrophysical Journal Letters, 862, L13. doi: 10.3847/2041-8213/aadlf5.
Taylor, B.J. (1996) Supermetallicity at the quarter-century mark: A conservative statistician's review of the evidence. The Astrophysical Journal Supplement, 102, 105.
Timmes, F.X., Woosley, S.E., and Weaver, T.A. (1995) Galactic chemical evolution: Hydrogen through zinc. The Astrophysical Journal Supplement Series, 98, 617–658.
Timmes, F.X., Woosley, S.E., Hartmann, D.H., and Hoffman, R.D. (1996) The production of ^{44}Ti and ^{60}Co in supernovae. The Astrophysical Journal, 464, 332–341.
Tominga, N., Umeda, H., and Nomoto, K. (2007) Supernova nucleosynthesis in population III 13-50 Msolar stars and abundance patterns of extremely metal-poor stars. The Astrophysical Journal, 660, 516–540.
Travaglio, C., Gallino, R., Amari, S., Zinner, E., Woosley, S., and Lewis, R.S. (1999) Low-density graphite grains and mixing in type II supernovae. The Astrophysical Journal, 510, 325–354.
Treffers, R., and Cohen, M. (1974) High-resolution spectra of cool stars in the 10- and 20-micron regions. The Astrophysical Journal, 188, 545–552.
Truran, J.W. and Heger, A. (2003) Origin of the elements. In H.D. Holland and K.K. Turekian, Eds., Treatise on Geochemistry, 1st ed., 1, 1–15. Elsevier.
Verchovsky, A.B., Fisenko, A.V., Semjonova, L.F., Bridges, J., Lee, M.R., and Wright, I.P. (2006) Nanodiamonds from AGB stars: A new type of presolar grain in meteorites. The Astrophysical Journal, 651, 481–490.
Vollmer, C., Hoppe, P., Brenker, F.E., and Hozapfel, C. (2007) Stellar $MgSiO_3$ perovskite: A shock-transformed stardust silicate found in a meteorite. The Astrophysical Journal, 666, L49–L52.
Vollmer, C., Hoppe, P., Stadermann, F.J., Floss, C., and Brenker, F.E. (2009) NanoSIMS analysis and Auger electron spectroscopy of silicate and oxide stardust from the carbonaceous chondrite Acfer 094. Geochimica et Cosmochimica Acta, 73, 7127–7149.
Vollmer, C., Hoppe, P., and Brenker, F.E. (2013) Transmission electron microscopy of Al-rich silicate stardust from asymptotic giant branch stars. The Astrophysical Journal, 769, 61 (8 pp).
Waters, L.B.F.M., Molster, F.J., de Jong, T., Beintema, D.A., Waelkens, C., and 32 others (1996) Mineralogy of oxygen-rich dust shells. Astronomy & Astrophysics, 315, L361-L364.
Wood, J.A., and Hashimoto, A. (1993) Mineral equilibrium in fractionated nebular systems. Geochimica et Cosmochimica Acta, 57, 2377–2388.
Woolf, N.J., and Ney, E.P. (1969) Circumstellar infrared emission from cool stars. The Astrophysical Journal, 155, L181.
Wopenka, B., Jadhav, M., and Zinner, E. (2011a) Raman analysis of high-density presolar graphite grains from the Orgueil carbonaceous chondrite. Lunar and Planetary Science Conference, 42, #1162.
Wopenka, B., Groopman, E., and Zinner, E. (2011b) Orgueil low-density presolar carbon ain't graphite but glassy carbon. Meteoritics & Planetary Science, 46, A252.
Yada, T., Floss, C., Stadermann, F.J., Zinner, E., Nakamura, T., Noguchi, T., and Lea, A.S. (2008) Stardust in Antarctic micrometeorites. Meteoritics & Planetary Science, 43, 1287–1298.
Yoneda, S., and Grossman, L. (1995) Condensation of CaO-MgO-Al_2O_3-SiO_2 liquids from cosmic gases. Geochimica et Cosmochimica Acta, 59, 3413–3444.
Zega, T.J., Alexander, C.M.O'D., Nittler, L.R., and Stroud, R.M. (2011) A transmission electron microscopy study of presolar hibonite. The Astrophysical Journal, 730, 83–93.
Zega, T.J., Nittler, L.R., Gyngard, F., Alexander, C.M.O'D., Stroud, R.M., and Zinner, E.K. (2014a) A transmission electron microscopy study of presolar spinel. Geochimica et Cosmochimica Acta, 124, 152–169.
Zega, T.J., Haenecour, P., Floss, C., and Stroud, R.M. (2014b) Extraction and analysis of presolar grains from the LAP 031117 CO3.0 chondrite. Lunar and Planetary Science Conference, 45, #2256.
Zega, T.J., Haenecour, P., Floss, C., and Stroud, R.M. (2015) Circumstellar magnetite from the LAP 031117 C03.0 chondrite. The Astrophysical Journal, 808, 55.
Zinner, E.K. (2014) Presolar grains. In A.M. Davis, H.D. Holland and K.K. Turekian, Eds., Treatise on Geochemistry, vol. 1., Meteorites, Comets, and Planets, 2nd ed., pp. 17–39. Oxford.
Zinner, E.K., Fahey, A.J., Goswami, J.N., Ireland, T.R., and McKeegan, K.D. (1986) Large ^{48}Ca anomalies associated with ^{50}Ti anomalies in Murchison and Murray hibonites. The Astrophysical Journal Letters, 311, L103–L107.
Zinner, E.K., Ming, T., and Anders, E. (1987) Large isotopic anomalies of Si, C, N, and noble gases in interstellar silicon carbide from the Murray meteorite. Nature, 330, 730–732.
Zinner, E.K., Amari, S., Wopenka, B., and Lewis, R.S. (1995) Interstellar graphite in meteorites: Isotopic compositions and structural properties of single graphite grains from Murchison. Meteoritics, 30, 209–226.
Zinner, E.K., Nittler, L.R., Gallino, R., Karakas, A.I., Lugaro, M., Straniero, O., and Lattanzio, J.C. (2006) Silicon and carbon isotopic ratios in AGB stars: SiC grain data, models, and the Galactic evolution of the Si isotopes. The Astrophysical Journal, 650, 350–373.
Zinner, E.K., Amari, S., Guinness, R., Jennings, C., Mertz, A.F., Nguyen, A.N., Gallino, R., Hoppe, P., Lugaro, M., Nittler, L.R., and Lewis, R.S. (2007) NanoSIMS isotopic analysis of small presolar grains: Search for Si_3N_4 grains from AGB stars and Al and Ti isotopic compositions of rare presolar SiC grains. Geochimica et Cosmochimica Acta, 71, 4786–4813.
Zinner, E.K., Moyniuer, F., and Stroud, R.M. (2011) Laboratory technology and cosmochemistry. Proceedings of the National Academy of Sciences, 108, 19,135–19,141.

Manuscript received June 23, 2019
Manuscript accepted December 2, 2019
Manuscript handled by Bruce Watson